Low-frequency two-dimensional linear instability of plane detonation *

Mark Short[1] and D. Scott Stewart[2]

[1]School of Mathematics, University of Bristol, Bristol BS8 1TW, U.K.
[2] Theoretical and Applied Mechanics, University of Illinois, Urbana, IL 61801, U.S.A.

Abstract

An analytical dispersion relation describing the low-frequency two-dimensional linear stability of a plane detonation wave characterized by a one-step Arrhenius reaction is derived using a normal mode approach and a combination of high-activation energy and Newtonian limit asymptotics, where the ratio of specific heats $\gamma \to 1$. The analysis relies on an assumption of a large activation energy in the plane steady-state detonation wave and a characteristic linear disturbance wavelength which is larger than the fire zone thickness. Newtonian limit asymptotics are employed to obtain a complete analytical description of the disturbance behaviour in the induction zone of the detonation wave. The analytical dispersion relation that is derived retains a dependence on the activation energy and demonstrates an excellent agreement with numerical solutions of the full linear stability problem for low-frequency, one- and two-dimensional disturbances even when the activation energy is only moderate. Moreover, the dispersion relation retains vitally important characteristics of the full problem such as stability of the detonation wave for decreasing activation energies or increasing overdrives. In addition, through a new detailed analysis of the behaviour of perturbations near the fire front, the present analysis is found to be equally valid for detonation waves travelling at the Chapman-Jouguet velocity or for detonation waves which are overdriven. It is found that in contrast to the standard imposition of a radiation or piston condition on acoustic disturbances in the equilibrium zone for overdriven waves, a compatibility condition on the perturbation jump conditions across the fire zone must be satisified for detonation waves propagating at the Chapman-Jouguet detonation velocity. An insight into the physical mechanisms of the one- and two-dimensional linear instability is also determined, and is found to involve an intricate coupling between acoustic and entropy wave propagation within the detonation wave.

1. Introduction

It has been well established experimentally and theoretically that plane, steady gaseous detonation waves are inherently unstable. Pulsating, bow shock detonation instabilities, with a one-dimensional character, have been observed off the forward surface of hypersonic spherical projectiles travelling in an explosive atmosphere (Alpert and Toong 1972). Numerical simulations of strictly one-dimensional, nominally steady, overdriven detonation for a standard model

*Submitted to the Journal of Fluid Mechanics, March 1996.

with a one-step Arrhenius reaction rate exhibit longitudinal pulsating instabilities (Fickett and Wood 1966, Bourlioux *et al.* 1991 and Quirk 1994). Two-dimensional unstable plane detonation waves prominently display a cellular instability that has an inherently different character than the pulsating one-dimensional instability. Experiments in gases show that cellular detonation is a complex multi-dimensional structure, with transverse shock waves propagating along the face of the lead shock (Strehlow 1970).

A model of detonation, defined by the reactive Euler equations with an ideal equation of state and a single exothermic reaction with Arrhenius kinetics, was used by Erpenbeck (1964) to study the stability of plane detonations. Subsequently, his model has become the standard one used by other researchers for the purpose of analytical and numerical studies of detonation stability and dynamics in terms of the parameters that define the steady state, such as the ratio of specific heats, the heat of combustion, the activation energy and steady detonation speed. The steady plane detonation structure of the standard model is the Zeldovich-Neumann-Döring (ZND) wave which is obtained by using the first integrals of mass, momentum and energy conservation in the reaction zone to substitute for the reaction progress variable in the rate equation, which in turn is solved for the spatial distribution of fuel (say) in the reaction zone.

The system of ordinary differential equations (ODEs) governing the stability of linear, normal mode, disturbances of the steady solutions have non-constant coefficients due to the spatial variation of the steady state. For the most general case, an exact analytical solution of the linear stability ODEs is not practically possible. Instead, a numerical treatment is required. The normal modes formulation and approach put forward by Lee and Stewart (1990) solves exactly (albeit numerically) the stability ODEs and provides a straightforward means to obtain exact solutions to the stability problem for the standard model. However, the numerical solutions do not provide a simple insight into the physical mechanisms that govern detonation instabilities.

A point of substantial interest in the more recent numerical studies of one-dimensional (1D) pulsating detonation wave propagation (Bourlioux *et al.* 1991, Quirk 1994 and Quirk and Short 1996) is that for steady detonation flows with parameters near those that define the linear neutral stability boundary, the pulsation period of the nonlinear oscillation agrees almost identically with the period of the lowest frequency linearly unstable mode. This agreement between the two periods is maintained even as the steady detonation parameters are varied substantially away from those corresponding to neutral stability towards greater instability. Thus even in the presence of several linearly unstable modes with larger growth rates, the lowest frequency mode appears to determine the period of the nonlinear pulsation of the unstable 1D detonation wave. Indeed Abouseif and Toong (1982) made similar observations and probably were the first to suggest that even for unstable detonations, the properties of the low-frequency linear spectra of unstable one-dimensional detonation waves could be used to predict the salient features of the acoustic mechanism of the low-frequency nonlinear pulsation.

Unlike the situation in 1D computations, accurate numerical simulation of two-dimensional (2D) detonation wave propagation is severely hampered by the extremely fine spatial and tem-

poral scales which characterize the intricate hydrodynamical and chemical coupling in multi-dimensional flow. Advances in 2D detonation computations for the standard model have been made though, most notably by Bourlioux and Majda (1992) and Quirk (1994,1995); the latter involves the essential use of highly sophisticated adaptive mesh refinement techniques. However it is not yet clear that a spatially resolved and wholly converged representation of two-dimensional cellular detonation has ever been carried out by any investigator. Thus conclusions concerning two-dimensional dynamics obtained from numerical simulation should be regarded as being less certain than similar ones made for one-dimensional simulations.

A widely-held premise has been that the spacing (or width) of the nonlinear detonation cells can be predicted by finding the linear disturbance wavelength that corresponds to the maximum unstable growth rate. However, in a recent exact treatment of two-dimensional plane detonation instability, Short and Stewart (1996) have found that the wavelength corresponding to the maximum unstable growth rate of the lowest frequency unstable mode offers a substantially better comparison with the cell sizes.

Indeed a similar observation can be inferred from the work of Yao and Stewart (1996) and Stewart *et al* (1996). Yao and Stewart, using combined limits of near Chapman-Jouguet (CJ) detonation velocity, large dimensionless activation energy and slow dynamic shock evolution measured on the time scale of particle passage through the reaction zone, have systematically derived an intrinsic evolution equation for the motion of the lead detonation shock. One of the essential new ingredients in the work is the inclusion of acoustic effects. Their shock dynamic equation is a relation between the normal shock velocity, the first and second time derivatives of the normal shock velocity, the shock curvature, and the first normal time derivative of the shock curvature. The Stewart-Yao shock evolution equation is a third-order in time, second-order in space, hyperbolic partial differential equation in the shock displacement, which when solved numerically, as described in Stewart *et al* (1996), produces the sustained cellular patterns observed in the experiments. Moreover, it was found that the cell-spacing could be reliably predicted by the wavelength of the neutrally stable low-frequency mode (Stewart *et al* 1996).

Thus there is a significant amount of evidence that in both 1D and 2D problems, there are a range of detonation parameters where a definitive link exists between the low-frequency and low wavenumber portions of the unstable linear spectra and the nonlinear mechanisms of detonation instability. Thus an analytically tractable theory of the *low-frequency* and *low wavenumber* linear instability of the plane steady detonation wave is desired. As such, we have been led to pursue rational asymptotic limits of the exact linear stability problem for the standard model, in limits suitable for gaseous detonation, to make improvements on and remove the deficiencies of some of the previous work in this direction.

The rational asymptotic approaches to the linear stability problem for the standard model are limited in number and thus far appear only in the works of Erpenbeck (1963), Buckmaster and Ludford (1987), Buckmaster (1989), Buckmaster and Neves (1988), Short (1996b) and Yao and Stewart (1996). All of the work mentioned involves the limit of a large activation energy, where

the steady detonation wave assumes the well-known square wave structure. The shock ignites the material and is followed by an induction zone of small reaction depletion. The induction zone has an a well-defined length $\tilde{L}^*$, and is followed by a thin reaction zone commonly referred to as the "fire". The fire is connected to a trailing, effectively inert equilibrium (or burnt) zone.

In one of the first modern uses of activation energy asymptotics, Erpenbeck (1963) presented the first rational investigation of the linear stability of detonation in the limit of large activation using a Laplace Transform formulation. It was demonstrated that Zaidel's (1961) *ad-hoc* stability model in which the steady state detonation structure is replaced by a piecewise constant structure possesses an infinite number of unstable modes whose growth rates increase with increasing frequency. Moreover, Erpenbeck (1963) was led to reject Zaidel's formulation due to the apparent non-existence of an assumed Laplace transform. Later, Buckmaster and Neves (1988) demonstrated using formal large activation energy asymptotics that the pathological spectrum determined by Zaidel (1961) is in fact representative of the linear stability spectrum for an unstable detonation wave in the limit of very large activation energies. This has also been verified numerically by Short (1996a). However, the work of Lee and Stewart (1990) established that for finite activation energies, sufficiently high-frequency disturbances are stable, and thus in general, the linear stability spectrum should possess a turning point as the frequency is increased.

The analysis of Buckmaster and Neves (1988) considered one-dimensional disturbances, where the disturbance frequency and growth rate was explicitly assumed to be $O(1)$ on the time-scale of acoustic passage across the induction zone $\tilde{L}^*/\tilde{c}_s^*$, where $\tilde{c}_s^*$ is the adiabatic post-shock sound speed. As mentioned above, Buckmaster and Neves found that the linear stability spectrum consisted of an infinite number of unstable oscillatory modes, whose growth rates increased monotonically with increasing frequency. Short (1996b) gave an analytical solution to the problem posed by Buckmaster and Neves through the use of the Newtonian limit where the ratio of specific heats $\gamma \to 1$. The analysis of Short (1996b) otherwise shares the same scalings as those used by Buckmaster and Neves (1988), but also includes two-dimensional disturbances in which in the characteristic disturbance wavenumber varies on a scale which is shorter or of the same order as the induction length. The analytical dispersion relation derived by Short (1996b) reproduces the one-dimensional results of Buckmaster and Neves almost identically and established the limit $\gamma \to 1$ as an effective tool in detonation stability studies.

The work found in Buckmaster and Ludford (1987) is concerned with two-dimensional, slowly-varying and small wavenumber disturbances. Specifically, the disturbances are taken to evolve on the time scale $\theta\tilde{L}^*/\tilde{c}_s^*$, where θ represents the non-dimensional large activation energy. The transverse disturbances are assumed to have a characteristic wavelength $\theta\tilde{L}^*$. They found a single non-oscillatory eigenvalue whose growth rate increases with increasing wavenumber. Buckmaster (1989) later extended the analysis of Buckmaster and Ludford (1987) to transverse disturbances which have a characteristic wavelength $O(\sqrt{\theta}\tilde{L}^*)$, and again found a single non-oscillatory unstable eigenvalue, but with growth rates which decrease as the wavenumber increase.

Yao and Stewart (1996) used a different asymptotic technique based on the method of successive approximations to derive their nonlinear evolution equation describing the unstable propagation of a Chapman-Jouguet detonation shock. The linear dispersion relation for the front equation leads to an approximation to the exact dispersion relation for the full system, where the activation energy appears in a natural way based on the assumption of the balance of certain dynamical terms that lead to well-posed solutions to the Stewart-Yao evolution equation. In particular, explicit algebraic expansions in the activation energy are not directly employed and subsequently their equation effectively represents what would be a composite expansion of a transient for the shock displacement, composed over a well-defined cycle of the dynamic evolution of the front. Indeed such an expansion must include more complex logarithmic dependence in general.

The main drawback with the previous high activation energy approaches, apart from that of Yao and Stewart (1996), is that activation energy scalings have been a priori attached to explicit algebraic expansions in the activation energy for the disturbance growth rates, frequencies and wavenumbers. This leads to dispersion relations that have a narrow range of validity. In our present work, we use a different asymptotic strategy that uses the limits of large activation energy to generate a limiting form of the stability problem that reflects the square wave structure, which is then solved analytically as opposed to numerically by using the limit $\gamma \to 1$. Moreover, in using this sequential-limit asymptotic analysis, the activation energy is found to be retained as a parameter in the dispersion relation.

The analysis proceeds as follows. First we derive the exact two-dimensional linear stability problem in its most general form without asymptotic simplification. The steady detonation state is expressed in its limiting form for large activation energy, consisting of a well-defined induction zone, thin fire zone and equilibrium zone structure. A stability problem for linear disturbances in the induction zone is then derived, in which terms which are explicitly $O(1/\theta)$ relative to the retained terms are omitted. Note that no assumptions regarding the growth rates, frequencies or wavenumbers of the disturbance are made at this stage. The linear stability problem in the induction zone is then solved in the limit $\gamma \to 1$, where the heat of combustion is assumed to be inversely proportion to $(\gamma - 1)$ so that the product of the heat of combustion time and the heat release is $O(1)$. This limit ensures that we are far away from a small heat-release limit.

We then derive a dispersion relation for all disturbances which have a characteristic wavelength larger than the nominally exponentially thin fire zone (which we define as *low-frequency*). The linearized shock relations are connected via an analytical solution of the induction zone to the fire. The fire location is determined so that an apparent singularity in the induction zone expansion is suppressed. This is achieved through a Lighthill straining of the induction zone coordinate. Since we confine our present investigations to low-frequency disturbances, the fire can be represented as a discontinuous Rankine-Hugoniot (RH) deflagration by its jump relations which connect the solution ahead of the fire to that behind. Finally a radiation condition is applied in the burnt or equilibrium zone, providing the extra homogeneous condition required

to specify the dispersion relation. Also, as well as deriving an analytical dispersion relation for overdriven detonation waves, a rational derivation of an analytical dispersion relation corresponding to CJ detonation waves is also given. We then show comparisons of our asymptotically derived results with numerical results for the exact spectra. Even for moderate activation energies, the comparison between the exact and asymptotic predictions are very close in both one- and two-dimensions and for all detonations speeds.

Our work also includes the important resolution of any remain concerns regarding the ill-posed nature of the linear stability of the CJ detonation wave. This is achieved through a detailed analysis of the jump conditions across the RH discontinuity and the nature of the perturbation behaviour in the burnt gas. For overdriven detonation waves, where the steady flow in the burnt gas is subsonic, the standard condition that specifies the dispersion relation is an acoustic radiation condition which prevents upstream propagation of disturbance from infinity. However, this choice is not unique in determining the burnt gas behaviour. For the CJ detonation wave, where the steady flow in the burnt gas is exactly sonic, we find that an acoustic radiation condition *must* be satisfied and since there is no choice on the behavior of the burnt zone conditions, the general perturbation jump conditions across the flame front are then degenerate. This leads to a compatibility condition on the jump conditions across the fire zone in order to determine the dispersion relation for CJ waves.

The remainder of the paper is as follows. In section 2 we describe the model equations and reaction rate law. In section 3 we describe the detonation structure in the limit of large activation energy. Section 4 states the exact linear stability problem. The approximation to the exact stability problem in the limit of large activation energy is stated in the induction zone, and is solved analytically by the use of the Newtonian limit, where $\gamma \to 1$. The Rankine-Hugoniot relations for the flame front perturbations are given and the acoustic properties of the equilibrium zone is discussed. Finally section 4 derives the asymptotic forms for the dispersion relation for both overdriven waves and CJ waves. Section 5 compares the prediction of the asymptotically derived results with numerical calculations of the exact stability problem.

2. Model

The equations describing the hydrodynamic evolution of a detonation wave are the reactive Euler equations,

$$\begin{gathered} \frac{D\rho}{Dt} + \rho \nabla . \mathbf{u} = 0, \quad \rho \frac{D\mathbf{u}}{Dt} = -\nabla p, \quad \frac{De}{Dt} + p\frac{D\rho^{-1}}{Dt} = 0, \\ \frac{DY}{Dt} = r, \quad r = r(p,\rho,Y), \quad e = e(p,\rho,Y), \end{gathered} \tag{1}$$

for density ρ, velocity $\mathbf{u}$, pressure p and reactant mass fraction Y. Here $Y = 1$ represents unreacted material while $Y = 0$ represents completely burnt material. The specific internal energy e and equation of state are taken to correspond to an ideal perfect gas, such that

$$e = \frac{p}{(\gamma - 1)\rho} + QY, \quad RT = \frac{p}{\rho}, \tag{2}$$

for temperature T, ratio of specific heats γ, chemical heat release factor Q and gas constant R. The rate law r is taken to be the one-step irreversible Arrhenius reaction,

$$r = -KY \exp\left(-\frac{E}{RT}\right), \tag{3}$$

where K is the Arrhenius pre-exponential factor and E is the activation energy of the reaction. Non-dimensional scales are chosen with reference to the one-dimensional, steady detonation wave. In particular, the density, temperature and velocity scales are the detonation shock density $\tilde{\rho}_s^*$, temperature $\tilde{T}_s^*$ and sound speed $\tilde{c}_s^*$ respectively. Here, and subsequently, we adopt the notation of a tilde $\tilde{}$ to refer to dimensional quantities, the superscript * to represent steady values, and the subscript s to correspond to the detonation shock values. The scaling of pressure is taken with respect to $\tilde{\rho}_s^* \tilde{c}_s^{*\,2}$, while the characteristic length scale $\tilde{L}^*$ is chosen as

$$\tilde{L}^* = \left(\frac{\tilde{c}_s^*}{\tilde{\mathcal{K}}}\right) \frac{\mathcal{K}}{\beta} \frac{e^\theta}{\theta}, \tag{4}$$

which is the steady induction zone length in the limit of large activation energy (Buckmaster and Ludford 1987). The non-dimensional activation energy θ and heat release β appearing in (4) are defined by

$$\theta = \frac{\tilde{E}}{\tilde{R}\tilde{T}_s^*}, \quad \beta = \frac{(\gamma-1)\tilde{Q}}{\tilde{c}_s^{*\,2}}, \tag{5}$$

while the constant $\mathcal{K}$ is given by

$$\mathcal{K} = \frac{M_s(M_s^2-1)}{(\gamma M_s^2 - 1)}, \tag{6}$$

where M_s is the steady, post-shock, particle Mach number, defined as

$$M_s = \frac{\tilde{u}_s^*}{\tilde{c}_s^*}, \tag{7}$$

where u_s^* is the dimensional post-shock particle velocity. It is also useful at this stage to define Erpenbeck's (1963) alternative definitions for the activation energy and heat release, which do not depend on the shock speed. These are

$$Q = \frac{\gamma\tilde{Q}}{\tilde{c}_0^{*\,2}}, \quad E = \frac{\gamma\tilde{E}}{\tilde{c}_0^{*\,2}}, \tag{8}$$

where $\tilde{c}_0^*$ is the pre-shock sound speed (the subscript 0 will be used in the following to denote the constant pre-shock state). The relationships between θ and E and β and Q are given by

$$\beta = \frac{(\gamma-1)}{\gamma} \frac{Q}{(\tilde{c}_s^{*\,2}/\tilde{c}_0^{*\,2})}, \quad \theta = \frac{E}{(\tilde{c}_s^{*\,2}/\tilde{c}_0^{*\,2})}, \tag{9}$$

where,

$$\frac{\tilde{c}_s^{*\,2}}{\tilde{c}_0^{*\,2}} = \frac{(2\gamma D^2 - 1 + \gamma)(2 + (\gamma-1)D^2)}{(\gamma+1)^2 D^2}, \tag{10}$$

and $D = \widetilde{D}/\tilde{c}_0^*$ is the propagation Mach number of the steady one-dimensional detonation relative to the upstream uniform pre-shock reactive atmosphere. Finally, the time scale is given by $\widetilde{L}^*/\tilde{c}_s^*$. With these scalings, the equations (1)–(3) can be written in the non-dimensional form,

$$\begin{gathered}\frac{D\rho}{Dt} + \rho\nabla.\mathbf{u} = 0, \quad \rho\frac{D\mathbf{u}}{Dt} = -\nabla p, \quad \rho\frac{DT}{Dt} = (\gamma-1)\frac{Dp}{Dt} - \beta\rho\frac{DY}{Dt}, \\ \frac{DY}{Dt} = r = -\frac{\mathcal{K}}{\theta\beta}Y\exp\left[\theta\left(1-\frac{1}{T}\right)\right], \quad T = \gamma p/\rho,\end{gathered} \tag{11}$$

where the convective derivative D/Dt is given by

$$\frac{D}{Dt} = \frac{\partial}{\partial t} + u\frac{\partial}{\partial n} + v\frac{\partial}{\partial y}, \tag{12}$$

for a horizontal velocity component u and horizontal cartesian co-ordinate n, that are in a frame of reference attached to the steady detonation shock, and a transverse velocity component and transverse cartesian co-ordinate given by v and y respectively.

In the following, we will assume the following asymptotic behaviour for θ and β, namely

$$\theta \gg 1, \quad \beta \sim O(1). \tag{13}$$

The scaling of the heat release factor β is chosen such that in the asymptotic limit where the specific heats ratio $\gamma \to 1$, we wish to maintain a strong, leading-order coupling between chemical and gasdynamic evolutions. It is emphasized that we are not concerned with a weak heat release limit.

3. Steady detonation structure

With a Mach number D relative to the upstream uniform reactive atmosphere, the overdrive f of the steady detonation is defined by,

$$f = (D/D_{CJ})^2, \tag{14}$$

where D_{CJ} is the Chapman-Jouguet Mach number at which $f = 1$, and is given by

$$D_{CJ} = \left[\left(1+\frac{(\gamma^2-1)}{\gamma}Q\right) + \sqrt{\left(1+\frac{(\gamma^2-1)}{\gamma}Q\right)^2 - 1}\right]^{1/2}, \tag{15}$$

for a given heat release Q. In a frame of reference attached to the steady detonation shock, such that

$$n = n^l - (\widetilde{D}/\tilde{c}_s^*)t, \tag{16}$$

where n^l denotes the lab-frame horizontal co-ordinate and the detonation structure lies in the region $n > 0$, the steady pressure, density, velocity and temperature variation through the wave

can be calculated from the Rankine-Hugoniot relations as

$$p^* = a + (\gamma^{-1} - a)\,(1 - bQ(1 - Y^*))^{\frac{1}{2}}, \quad u^* = \frac{(1 - \gamma p^*)}{\gamma M_s} + M_s, \quad v^* = 0,$$
$$\rho^* = \frac{M_s}{u^*}, \quad T^* = \gamma P^*/\rho^*, \tag{17}$$

where

$$M_s = \left[\frac{2 + (\gamma - 1)D^2}{2\gamma D^2 - (\gamma - 1)}\right]^{\frac{1}{2}}, \quad a = \frac{\gamma^{-1}(1 + \gamma D^2)}{(2\gamma D^2 + 1 - \gamma)}, \quad b = \frac{2(\gamma^2 - 1)D^2}{\gamma(D^2 - 1)^2}. \tag{18}$$

It is easily verified that when $D = D_{CJ}$ and the reaction is complete, i.e. when $Y^* = 0$ the flow in the burnt gas is exactly sonic. In order to complete the description of the steady detonation structure, the distribution of the reactant mass fraction must be determined through the integral equation,

$$n = -\frac{\beta\theta}{\mathcal{K}} \int_1^{Y^*} \frac{u^*}{Y^*} \exp\left[-\theta\left(1 - \frac{1}{T^*}\right)\right] \mathrm{d}Y^*. \tag{19}$$

3(a) Square-wave structure

In the asymptotic limit of high activation energy where $\theta \gg 1$, the steady detonation assumes the form of a square wave detonation consisting of an induction zone with weak chemical heat release, terminated by a thin fire zone leading into a uniform chemical equilibrium (or burnt) state. As in Buckmaster and Ludford (1987) and Short (1996), the induction state is determined by expanding the variables ρ, p, u, v, T and Y in the form

$$\mathbf{z}^* = \mathbf{z}_s^* + \frac{1}{\theta}\mathbf{z}_1^*(n) + O\left(\frac{1}{\theta^2}\right), \tag{20}$$

where

$$\mathbf{z} = [\rho,\ u,\ v,\ p,\ T,\ Y]^{\mathrm{T}}, \quad \mathbf{z}_s^* = [1,\ M,\ 0,\ 1/\gamma,\ 1,\ 1]^{\mathrm{T}}. \tag{21}$$

In the definition of $\mathbf{z}$ we note a dependence between T, p and ρ : however, it is convenient to retain $\mathbf{z}$ in this form for ease of computation later. By substituting the expansion (20) into (17) and (19), it can be verified that the deviation of the steady induction solution from the post-shock state is determined by the perturbations,

$$T_1^* = -\ln(1 - n), \quad p_1^* = -\frac{M_s^2}{(\gamma M_s^2 - 1)}\ln(1 - n), \quad u_1^* = \frac{M_s}{(\gamma M_s^2 - 1)}\ln(1 - n), \quad v_1^* = 0,$$
$$\rho_1^* = -\frac{1}{(\gamma M_s^2 - 1)}\ln(1 - n), \quad Y_1^* = \frac{1}{\beta}\frac{(M_s^2 - 1)}{(\gamma M_s^2 - 1)}\ln(1 - n). \tag{22}$$

At $n = 1$, the steady induction zone perturbation solutions $\mathbf{z}_1^*(n)$ are logarithmically singular rendering the expansion (20) non-uniform. A thin fire zone of rapid reaction, in which the steady variables change by $O(1)$ amounts, and a thin relaxation zone, in which the steady variables

deviate by an $O(\theta^{-1})$ amount from their final state, then connect the end of the induction zone to the chemically burnt (or equilibrium) regime. In the standard way, the structure of the fire zone could easily be determined in terms of the re-scaling variable,

$$\sigma = -\ln(1-n), \tag{23}$$

but since we restrict our present discussions to perturbations with a long wavelength compared to the fire thickness, the fire and relaxation zones can be simply treated as a discontinuous Rankine-Hugoniot deflagration. A schematic of the steady detonation structure in the limit of large activation energy is given in figure 1.

4. Linear Stability Analysis

The general linear stability problem is formulated by first defining a shock-attached co-ordinate system,

$$x = n - h(y,t), \tag{24}$$

where $h(y,t)$ is the shock displacement in relation to the steady shock location at $n=0$ and $x=0$ denotes the shock position in the new co-ordinate system. The governing equations (11) become in matrix form,

$$\mathbf{z}_{,t} + \mathbf{A}\cdot\mathbf{z}_{,x} + \mathbf{B}\cdot\mathbf{z}_{,y} - h_{,t}\mathbf{z}_{,x} - h_{,y}\mathbf{B}\cdot\mathbf{z}_{,x} = \mathbf{c}, \tag{25}$$

where the chemical matrix $\mathbf{c}$ is defined as

$$\mathbf{c} = [0,\ 0,\ 0,\ -\beta\rho r,\ -\gamma\beta r,\ \ r]^{\mathrm{T}}, \tag{26}$$

and

$$\mathbf{A} = \begin{bmatrix} u & \rho & 0 & 0 & 0 & 0 \\ 0 & u & 0 & 1/\rho & 0 & 0 \\ 0 & 0 & u & 0 & 0 & 0 \\ 0 & \gamma p & 0 & u & 0 & 0 \\ 0 & (\gamma-1)T & 0 & 0 & u & 0 \\ 0 & 0 & 0 & 0 & 0 & u \end{bmatrix}, \quad \mathbf{B} = \begin{bmatrix} v & 0 & \rho & 0 & 0 & 0 \\ 0 & v & 0 & 0 & 0 & 0 \\ 0 & 0 & v & 1/\rho & 0 & 0 \\ 0 & 0 & \gamma p & v & 0 & 0 \\ 0 & 0 & (\gamma-1)T & 0 & v & 0 \\ 0 & 0 & 0 & 0 & 0 & v \end{bmatrix}. \tag{27}$$

We now seek to determine the stability of the steady detonation wave to small two-dimensional linear perturbations by expanding the variables ρ, p, u, v, T and Y in the normal mode form,

$$\mathbf{z} = \mathbf{z}^*(x) + \mathbf{z}'(x)e^{\lambda t}e^{iky}, \tag{28}$$

where the superscript $'$ is used to represent an infinitesimal perturbation quantity. The complex growth rate is given by λ, where $\mathrm{Re}(\lambda)$ defines the real growth rate, $\mathrm{Im}(\lambda)$ the frequency and k the wavenumber of the disturbance. The matrix $\mathbf{z}'(x)$ describes the spatial structure of the perturbation eigenfunctions in the displaced flow. The shock displacement $h(y,t)$ is expanded as

$$h = h' e^{\lambda t} e^{iky}, \tag{29}$$

where h' is a constant. By substituting expansions (28) and (29) into (25), the linear perturbation equations are,

$$\lambda \mathbf{z}' + \mathbf{A}^* \cdot \mathbf{z}'_{,x} + ik\mathbf{B}^* \cdot \mathbf{z}' + (\mathbf{C}^*_g - \mathbf{C}^*_{ch}) \cdot \mathbf{z}' - \lambda h' \mathbf{z}^*_{,x} - ikh' \mathbf{B}^* \cdot \mathbf{z}^*_{,x} = 0, \tag{30}$$

where

$$\mathbf{C}^*_g = \begin{bmatrix} u_{,x} & \rho_{,x} & 0 & 0 & 0 & 0 \\ -p_{,x}/\rho^2 & u_{,x} & 0 & 0 & 0 & 0 \\ 0 & 0 & 0 & 0 & 0 & 0 \\ 0 & p_{,x} & 0 & \gamma u_{,x} & 0 & 0 \\ 0 & T_{,x} & 0 & 0 & (\gamma-1)u_{,x} & 0 \\ 0 & Y_{,x} & 0 & 0 & 0 & u_{,x} \end{bmatrix}^*, \tag{31}$$

is a matrix of gasdynamic origin and $\mathbf{C}^*_{ch}$ is a matrix of chemical origin, such that

$$\mathbf{C}^*_{ch} = -\frac{\mathcal{K}}{\beta} r_T \begin{bmatrix} 0 & 0 & 0 & 0 & 0 & 0 \\ 0 & 0 & 0 & 0 & 0 & 0 \\ 0 & 0 & 0 & 0 & 0 & 0 \\ -Y/\theta & 0 & 0 & 0 & -\rho\beta Y/T^2 & -\beta\rho/\theta \\ 0 & 0 & 0 & 0 & -\gamma\beta Y/T^2 & -\gamma\beta/\theta \\ 0 & 0 & 0 & 0 & Y/T^2 & 1/\theta \end{bmatrix}^*, \tag{32}$$

where

$$r_T = \exp\left[\theta\left(1 - \frac{1}{T}\right)\right]. \tag{33}$$

The linearized shock conditions for the perturbation variables are determined from the perturbed Rankine-Hugoniot relations across the detonation shock, which can be solved in terms of the normal mode perturbation expansions (28) and (29) as,

$$\rho' = \lambda h' \kappa_\rho, \quad u' = \lambda h' \kappa_u, \quad v' = ikh' \kappa_v, \quad p' = \lambda h' \kappa_p, \quad T' = (\gamma-1)\lambda h' \kappa_T, \quad Y' = 0, \tag{34}$$

where

$$\begin{aligned}
\kappa_\rho &= \left[\frac{M_s}{(M_s^2-1)}\frac{(\mu-1)}{\mu}\left[2-(\gamma-1)(\mu-1)\right]\right], \\
\kappa_u &= \left[\frac{1}{(M_s^2-1)}\frac{(\mu-1)}{\mu}\left[-1-(1-(\gamma-1)(\mu-1))M_s^2\right]\right], \\
\kappa_v &= \left[M_s(\mu-1)\right], \\
\kappa_p &= \left[\frac{M_s}{(M_s^2-1)}\frac{(\mu-1)}{\mu}\left[2-(\gamma-1)(\mu-1)M_s^2\right]\right], \\
\kappa_T &= \left[\frac{M_s}{(M_s^2-1)}\frac{(\mu-1)}{\mu}\left[2+(\mu-1)(1-\gamma M_s^2)\right]\right],
\end{aligned} \tag{35}$$

and

$$\mu = \frac{\tilde{\rho}_s^*}{\tilde{\rho}_0^*} = \frac{\tilde{u}_s^*}{\tilde{u}_0^*} = \frac{(\gamma+1)D^2}{2+(\gamma-1)D^2}, \tag{36}$$

is the ratio of the shocked gas density to the unperturbed pre-shock gas density. Thus the general linear stability problem is obtained by solving equations (30) subject to the shock conditions (34), plus an additional condition on the perturbations. For overdriven detonation waves ($f > 1$), this condition can, for example, take the form of either a radiation or piston condition on acoustic disturbances in the burnt gas. This condition, and the radiation condition that is appropriate for CJ detonations, is discussed in detail in sections 4(f) and 4(g) below. We now seek a new asymptotic solution to the general stability problem by successively employing the limits of high-activation energy and the Newtonian limit in which the specific heats ratio $\gamma \to 1$.

4(a) Perturbation equations in the induction zone (IZ)

An approximation of the exact linear stability problem (30) is now made, based first on the limit of large activation energy. In this limit, the steady solution in the induction zone (IZ) is given by expansion (20) with solution (22), and correspondingly the matrices $\mathbf{A}^*$, $\mathbf{B}^*$, $\mathbf{C}_g^*$, $\mathbf{C}_{ch}^*$ and $\mathbf{z}^*$ have the following asymptotic form in the IZ:

$$\begin{gathered}
\mathbf{A}^*(x;\theta) = \mathbf{A}_0^* + \frac{1}{\theta}\mathbf{A}_1^*(x), \quad \mathbf{B}^*(x;\theta) = \mathbf{B}_0^* + \frac{1}{\theta}\mathbf{B}_1^*(x), \quad \mathbf{C}_{ch}^* = (\mathbf{C}_{ch})_0^*(x) + \frac{1}{\theta}(\mathbf{C}_{ch})_1^*(x), \\
\mathbf{C}_g^*(x;\theta) = \frac{1}{\theta}(\mathbf{C}_g)_1^*(x), \quad \mathbf{z}^*(x;\theta) = \mathbf{z}_s^* + \frac{1}{\theta}\mathbf{z}_1^*(x),
\end{gathered} \tag{37}$$

where

$$\mathbf{A}_0^* = \begin{bmatrix} M_s & 1 & 0 & 0 & 0 & 0 \\ 0 & M_s & 0 & 1 & 0 & 0 \\ 0 & 0 & M_s & 0 & 0 & 0 \\ 0 & 1 & 0 & M_s & 0 & 0 \\ 0 & (\gamma-1) & 0 & 0 & M_s & 0 \\ 0 & 0 & 0 & 0 & 0 & M_s \end{bmatrix}, \quad \mathbf{B}_0^* = \begin{bmatrix} 0 & 0 & 1 & 0 & 0 & 0 \\ 0 & 0 & 0 & 0 & 0 & 0 \\ 0 & 0 & 0 & 1 & 0 & 0 \\ 0 & 0 & 1 & 0 & 0 & 0 \\ 0 & 0 & (\gamma-1) & 0 & 0 & 0 \\ 0 & 0 & 0 & 0 & 0 & 0 \end{bmatrix}, \tag{38}$$

and

$$(\mathbf{C}_{ch})_0^*(x) = -\frac{\mathcal{K}}{\beta(1-x)} \begin{bmatrix} 0 & 0 & 0 & 0 & 0 & 0 \\ 0 & 0 & 0 & 0 & 0 & 0 \\ 0 & 0 & 0 & 0 & 0 & 0 \\ 0 & 0 & 0 & 0 & -\beta & 0 \\ 0 & 0 & 0 & 0 & -\gamma\beta & 0 \\ 0 & 0 & 0 & 0 & 1 & 0 \end{bmatrix}. \tag{39}$$

Thus the matrices $\mathbf{A}^*$ and $\mathbf{B}^*$ are constant to leading order in the induction zone in an expansion in θ^{-1}, while the matrices $\mathbf{C}_g^*$ and $\mathbf{z}_{,x}^*$ are $O(1/\theta)$. The chemical perturbation matrix $(\mathbf{C}_{ch})_o^*(x)$ depends on the spatially varying steady induction zone structure, and reflects the singular nature of the induction zone structure near the flame front. The expansions (37) are now substituted into (30) and terms which are explicitly $O(1/\theta)$ are neglected, whereupon the perturbation equations (30) reduce to a system involving the standard set of linearized acoustic equations in an inert medium with a chemical forcing term which depends on the temperature perturbation and the steady induction zone solution. Specifically, the perturbation equations

which are valid in the induction zone can be written as

$$\begin{aligned}
\lambda u' + M_s \frac{du'}{dx} + \frac{dp'}{dx} &= 0, \\
\lambda v' + M_s \frac{dv'}{dx} + ikp' &= 0, \\
\lambda p' + M_s \frac{dp'}{dx} + \frac{du'}{dx} + ikv' &= \mathcal{K} \frac{T'}{1-x}, \\
\lambda T' + M_s \frac{dT'}{dx} + (\gamma - 1)\left(\frac{du'}{dx} + ikv'\right) &= \gamma \mathcal{K} \frac{T'}{1-x}, \\
\lambda Y' + M_s \frac{dY'}{dx} &= -\frac{\mathcal{K}}{\beta} \frac{T'}{1-x}, \\
\rho' &= \gamma p' - T'.
\end{aligned} \tag{40}$$

At this stage we make the important remark that the equations (40) have been derived based on a large activation energy assumption on the steady state. As such, the induction zone perturbation eigenfunctions equations (40) are valid to leading order for any $O(1)$ values of λ or k large or small. The only requirement on the validity of the equations (40) is that the activation energy be moderately large, so that the state in the IZ away from the fire is nearly uniform. In fact, these equations correspond to a linearized two-dimensional version of Clarke's equations (1985). We shall now proceed to provide a complete asymptotic solution for equations (40) through the use of Newtonian limit asymptotics.

4(b) Solution of the temperature perturbation in the induction zone in the limit $\gamma \to 1$

It is well known that a solution of the one-dimensional version of Clarke's equations (1985) is available in the Newtonian limit, in which the ratio of specific heats is close to unity (Blythe and Crighton 1989). In a recent work by Short (1996b), this limit was used to describe the behaviour of the linear stability spectrum through equations (40) when λ was explicitly order one, $k \sim O(1)$ and $\theta \to \infty$. In this parameter regime, a solution to $O(\gamma - 1)$ for T' was all that was required to determine the spectrum and the excellent agreement with the numerical results of Buckmaster and Neves (1988) established this limit as an effective tool in detonation stability problems. We shall next proceed to significantly generalize and extend this technique to provide a general solution to the linear stability problem for low-frequency disturbances, which retains the activation energy as an explicit parameter in the problem, in contrast to the previous studies of Buckmaster and Ludford (1987), Buckmaster (1988) and Short (1996b). To proceed, it is now assumed that the ratio of the isothermal to isentropic sound speeds is close to unity, which for a perfect gas, is equivalent to assuming that the ratio of the specific heats is close to unity, i.e.

$$(\gamma - 1) \ll 1. \tag{41}$$

In adopting this procedure, we have thus chosen to undertake a sequential limiting process in determining the solution in the induction zone, where we let $\theta \to \infty$ followed by $\gamma \to 1$, so that the eigenfunction approximation in the IZ to the order we are concerned is valid provided

$$\frac{1}{\theta} \ll (\gamma - 1) \ll 1. \tag{42}$$

The behaviour of the perturbation eigenfunctions in the induction zone in the Newtonian limit are now found by defining eigenfunction expansions for ρ', u', v', p', Y' and T' as

$$\mathbf{z}'(x) = \mathbf{z}'_0(x) + (\gamma - 1)\mathbf{z}'_1(x) + \cdots, \tag{43}$$

and an eigenvalue expansion for λ as

$$\lambda = \lambda_0 + (\gamma - 1)\lambda_1 + \cdots. \tag{44}$$

Substituting expansions (43) and (44) into the first five of equations (40), the leading-order eigenfunction equations become,

$$\begin{gathered}
\lambda_0 u'_0 + M_s \frac{du'_0}{dx} + \frac{dp'_0}{dx} = 0, \quad \lambda_0 v'_0 + M_s \frac{dv'_0}{dx} + ikp'_0 = 0, \\
\lambda_0 p'_0 + M_s \frac{dp'_0}{dx} + \frac{du'_0}{dx} + ikv'_0 = \frac{M_s}{(1-x)} T'_0, \\
\lambda_0 T'_0 + M_s \frac{dT'_0}{dx} = \frac{M_s}{(1-x)} T'_0, \quad \lambda_0 Y'_0 + M_s \frac{dY'_0}{dx} = -\frac{M_s}{\beta(1-x)} T'_0,
\end{gathered} \tag{45}$$

where

$$\mathcal{K} = \frac{(M_s^2 - 1)}{(\gamma M_s^2 - 1)} = 1 + O(\gamma - 1). \tag{46}$$

Changes in the leading order temperature and reactant mass fraction perturbations are determined along particle paths only and are independent of changes in the leading order velocity or pressure perturbations. Under the expansions (43) and (44), the equations (45) are subject to the leading-order shock relations at $x = 0$ obtained from (34) as,

$$T'_0(0) = 0, \quad Y'_0(0) = 0, \quad p'_0(0) = \lambda_0 h' \kappa_p, \quad u'_0(0) = \lambda_0 h' \kappa_u, \quad v'_0(0) = ikh' \kappa_v, \tag{47}$$

where the coefficients κ_p, κ_u and κ_v are treated as known $O(1)$ constants. The fourth of equations (45) is integrated to give the solution

$$T'_0 = \frac{A}{1-x} e^{-\lambda_0 x / M_s}, \tag{48}$$

for constant A. Application of the first of boundary conditions (47) shows that to leading order in the expansions (43), $A = 0$ and the temperature perturbation within the induction zone must be set everywhere to zero, i.e.

$$T'_0 = 0. \tag{49}$$

Also, solving the last of equations (45) with the second of shock conditions (47) gives,

$$Y_0' = 0, \tag{50}$$

i.e. the reactant perturbation is everywhere zero in the induction zone. Thus, to leading order in the Newtonian limit, both the temperature and reactant mass fraction changes along particle paths are zero.

With (49), the first three of equations (45) determine the leading order pressure and velocity perturbations in the induction zone. Since $T_0' = 0$ and $Y_0' = 0$ there is no chemical forcing term in the third of equations (45) and the first three of equations (45) reduce simply to the standard equations of linearized acoustics, with the solution

$$\begin{aligned} p_0' &= \frac{(\lambda_0 - \lambda^{(2)} M_s)}{\lambda^{(2)}} A_1 e^{-\lambda^{(2)} x} + \frac{(\lambda_0 - \lambda^{(3)} M_s)}{\lambda^{(3)}} A_2 e^{-\lambda^{(3)} x}, \\ u_0' &= \frac{ikA_3}{\lambda^{(1)}} e^{-\lambda^{(1)} x} + A_1 e^{-\lambda^{(2)} x} + A_2 e^{-\lambda^{(3)} x}, \\ v_0' &= A_3 e^{-\lambda^{(1)} x} - \frac{ikA_1}{\lambda^{(2)}} e^{-\lambda^{(2)} x} - \frac{ikA_2}{\lambda^{(3)}} e^{-\lambda^{(3)} x}. \end{aligned} \tag{51}$$

The double eigenvalue

$$\lambda^{(1)} = \frac{\lambda_0}{M_s}, \tag{52}$$

corresponds to vorticity and entropy wave propagation in the induction zone and

$$\lambda^{(2,3)} = \frac{1}{(M_s^2 - 1)} (M_s \lambda_0 \pm \sqrt{\lambda_0^2 - (M_s^2 - 1)k^2}), \tag{53}$$

corresponds to acoustic wave propagation in the induction zone. The root $\lambda^{(3)}$ corresponds to backward facing characteristic paths which propagate changes at the shock to the fire zone, while the root $\lambda^{(2)}$ corresponds to forward facing characteristics connecting changes at the flame front to the shock wave. Thus to leading order in the Newtonian limit, the acoustic pressure and velocity disturbances propagate information around the induction zone uninfluenced by perturbations in the chemical reaction rate. However, as we shall see below, the role of these acoustic changes is to force $O(\gamma - 1)$ changes in the induction temperature perturbation variable which, when coupled with $O(\gamma - 1)$ in the perturbation shock temperature, lead directly to a displacement of the fire position relative to its steady value $n = 1$. From the shock conditions

(47), the coefficients A_1, A_2 and A_3 are determined as

$$\begin{aligned}
A_1 &= \left[\left(\frac{\lambda^{(1)}-\lambda^{(3)}}{\lambda^{(3)}}\right)(M_s\lambda^{(1)}\kappa_u+\frac{k^2}{\lambda^{(1)}}\kappa_v)-\left(1-\frac{k^2}{\lambda^{(1)}\lambda^{(3)}}\right)\lambda^{(1)}\kappa_p\right]h' \Big/ \\
&\quad \left[\left(1-\frac{k^2}{\lambda^{(1)}\lambda^{(2)}}\right)\left(\frac{\lambda^{(1)}-\lambda^{(3)}}{\lambda^{(3)}}\right)-\left(1-\frac{k^2}{\lambda^{(1)}\lambda^{(3)}}\right)\left(\frac{\lambda^{(1)}-\lambda^{(2)}}{\lambda^{(2)}}\right)\right], \\
A_2 &= \left[\left(\frac{\lambda^{(1)}-\lambda^{(2)}}{\lambda^{(2)}}\right)(M_s\lambda^{(1)}\kappa_u+\frac{k^2}{\lambda^{(1)}}\kappa_v)-\left(1-\frac{k^2}{\lambda^{(1)}\lambda^{(2)}}\right)\lambda^{(1)}\kappa_p\right]h' \Big/ \\
&\quad \left[\left(1-\frac{k^2}{\lambda^{(1)}\lambda^{(3)}}\right)\left(\frac{\lambda^{(1)}-\lambda^{(2)}}{\lambda^{(2)}}\right)-\left(1-\frac{k^2}{\lambda^{(1)}\lambda^{(2)}}\right)\left(\frac{\lambda^{(1)}-\lambda^{(3)}}{\lambda^{(3)}}\right)\right], \\
A_3 &= ikh'\kappa_v+\frac{ikA_1}{\lambda^{(2)}}+\frac{ikA_2}{\lambda^{(3)}}.
\end{aligned} \tag{54}$$

The equation for $T_1'(x)$ becomes,

$$\lambda_0 T_1' + M_s\frac{\mathrm{d}T_1'}{\mathrm{d}x}+\frac{\mathrm{d}u_0'}{\mathrm{d}x}+ikv_0' = \frac{M_s}{(1-x)}T_1', \tag{55}$$

which is obtained by substituting expansions (43) and (44) into the fourth of equations (40) and collecting terms of $O(\gamma-1)$. Thus T_1' is explicitly dependent on the propagation of the leading-order non-forced acoustic disturbances around the IZ. The boundary condition for T_1' at $x=0$ is obtained from the shock relations (34) as,

$$T_1'(0) = \lambda_0 h'\kappa_T, \tag{56}$$

so that T_1' also depends on changes at the shock front which are propagated along particle paths from the shock into the induction zone. The solution of equation (55) is determined to be,

$$\begin{aligned}
T_1' &= \frac{1}{1-x}\left[\frac{\alpha_1}{(\lambda^{(2)}-\lambda^{(1)})}e^{\lambda^{(2)}(1-x)}+\frac{\alpha_2}{(\lambda^{(3)}-\lambda^{(1)})}e^{\lambda^{(3)}(1-x)}+A_4e^{\lambda^{(1)}(1-x)}\right] \\
&\quad -\alpha_1e^{\lambda^{(2)}(1-x)}-\alpha_2e^{\lambda^{(3)}(1-x)},
\end{aligned} \tag{57}$$

where

$$\begin{aligned}
\alpha_1 &= \frac{A_1}{M_s(\lambda^{(2)}-\lambda^{(1)})}\left(\lambda^{(2)}-\frac{k^2}{\lambda^{(2)}}\right)e^{-\lambda^{(2)}}, \\
\alpha_2 &= \frac{A_2}{M_s(\lambda^{(3)}-\lambda^{(1)})}\left(\lambda^{(3)}-\frac{k^2}{\lambda^{(3)}}\right)e^{-\lambda^{(3)}}, \\
A_4 &= \left[M_s\lambda^{(1)}h'\kappa_T-\alpha_1\left(\frac{1}{(\lambda^{(2)}-\lambda^{(1)})}-1\right)e^{\lambda^{(2)}}-\alpha_2\left(\frac{1}{(\lambda^{(3)}-\lambda^{(1)})}-1\right)e^{\lambda^{(3)}}\right]e^{-\lambda^{(1)}}.
\end{aligned} \tag{58}$$

Thus the solution (57) emphasizes that T_1' depends equally on the leading order acoustic wave propagation along the characteristic paths corresponding to $\lambda^{(2)}$ and $\lambda^{(3)}$ and the $O(\gamma-1)$ changes in the perturbation shock temperature which are propagated along the particle paths

corresponding to $\lambda^{(1)}$. This interactive coupling between acoustic wave propagation and entropy changes results in a perturbation of the fire position relative to its steady position due to the presence of a pole singularity in (57) as $x \to 1$. We will now demonstrate how changes in $T'(x)$ at $O(\gamma-1)$ lead to $O(\gamma-1)$ changes in the chemical reaction rate in the IZ, which then force $O(\gamma-1)$ changes in $p'(x)$, $u'(x)$ and $v'(x)$.

4(c) Solution of the reactant mass fraction, pressure and velocity perturbations in the induction zone to $O(\gamma-1)$.

Having determined the solution of the temperature perturbation $T'(x)$ to $O(\gamma-1)$, it transpires that solutions for $Y'(x)$, $p'(x)$, $u'(x)$, $v'(x)$ and $\rho'(x)$ which are correct to $O(\gamma-1)$ can be determined directly from equations (40) without explicit need to continue with the above expansion procedure. Thus, with

$$T'(x) = (\gamma-1)T_1'(x), \tag{59}$$

the reactant perturbation equation becomes,

$$Y_x' + \lambda^{(1)}Y' = -\frac{(M_s^2-1)T'(x)}{\beta(\gamma M_s^2-1)(1-x)}, \tag{60}$$

which is a simple, chemically-forced, linear advection equation. Thus the presence of a $O(\gamma-1)$ temperature perturbation change leads to a $O(\gamma-1)$ perturbation in the chemical reaction rate, which in turn forces a $O(\gamma-1)$ change in the reactant mass fraction. The solution subject to the shock condition $Y'(0)=0$ is,

$$Y'(x) = (\gamma-1)Y_1'(x), \tag{61}$$

where

$$\begin{aligned} Y_1'(x) \;=\; & -\frac{(M_s^2-1)}{\beta(\gamma M_s^2-1)(1-x)}\left[\frac{\alpha_1 e^{\lambda^{(2)}(1-x)}}{(\lambda^{(2)}-\lambda^{(1)})}+\frac{\alpha_2 e^{\lambda^{(3)}(1-x)}}{(\lambda^{(3)}-\lambda^{(1)})}+A_4 e^{\lambda^{(1)}(1-x)}\right] \\ & +A_5 e^{-\lambda^{(1)}x}, \end{aligned} \tag{62}$$

where

$$A_5 = \frac{(M_s^2-1)}{\beta(\gamma M_s^2-1)}\left[\frac{\alpha_1}{(\lambda^{(2)}-\lambda^{(1)})}e^{\lambda^{(2)}}+\frac{\alpha_2}{(\lambda^{(3)}-\lambda^{(1)})}e^{\lambda^{(3)}}+A_4 e^{\lambda^{(1)}}\right]. \tag{63}$$

The pressure perturbation can now be determined through the equation,

$$(M_s^2-1)\frac{d^2p'}{dx^2}+2M_s\lambda\frac{dp'}{dx}+(\lambda^2+k^2)p' = \frac{M_s(M_s^2-1)}{(\gamma M_s^2-1)}\left[M_s\frac{d}{dx}\left[\frac{T'}{1-x}\right]+\frac{\lambda T'}{1-x}\right] \tag{64}$$

which represents the standard second-order linear acoustic pressure disturbance equation with a chemical forcing term. With $p'(x)$ known, the two velocity perturbations are then determined as

$$u' = -\frac{e^{-\lambda^{(1)}x}}{M_s}\int\left[\frac{dp'}{dx}\right]e^{\lambda^{(1)}x}\,\mathrm{dx}+\frac{ik}{\lambda^{(1)}}C_3 e^{-\lambda^{(1)}x}, \tag{65}$$

and

$$v' = -\frac{ik}{M_s} e^{-\lambda^{(1)}x} \int p' e^{\lambda^{(1)}x}\, \mathrm{dx} + C_3 e^{-\lambda^{(1)}x}, \tag{66}$$

where C_3 is a constant which is to be determined from the shock conditions (34). Thus the presence of the $O(\gamma-1)$ temperature perturbation change, also directly forces a $O(\gamma-1)$ change in the pressure and velocity perturbations relative to the chemically uninfluenced propagation of pressure and velocity disturbances around the IZ at leading order in the Newtonian limit expansion. The full pressure perturbation equation (64) is,

$$\begin{aligned}(M_s^2-1)\frac{d^2p'}{dx^2} + 2M_s\lambda\frac{dp'}{dx} + (\lambda^2+k^2)p' = (\gamma-1)\frac{M_s(M_s^2-1)}{(\gamma M_s^2-1)} \\ \times\left\{\frac{2M_s}{(1-x)^3}\left[\frac{\alpha_1 e^{\lambda^{(2)}(1-x)}}{(\lambda^{(2)}-\lambda^{(1)})} + \frac{\alpha_2 e^{\lambda^{(3)}(1-x)}}{(\lambda^{(3)}-\lambda^{(1)})} + A_4 e^{\lambda^{(1)}(1-x)}\right]\right. \\ -\frac{2M_s}{(1-x)^2}\left[\alpha_1 e^{\lambda^{(2)}(1-x)} + \alpha_2 e^{\lambda^{(3)}(1-x)}\right] \\ \left.+\frac{M_s}{(1-x)}\left[\alpha_1 e^{\lambda^{(2)}(1-x)}(\lambda^{(2)}-\lambda^{(1)}) + \alpha_2 e^{\lambda^{(3)}(1-x)}(\lambda^{(3)}-\lambda^{(1)})\right]\right\}\end{aligned} \tag{67}$$

which has the general solution,

$$p'(x) = M_s\frac{(\lambda^{(1)}-\lambda^{(2)})}{\lambda^{(2)}}C_1 e^{-\lambda^{(2)}x} + M_s\frac{(\lambda^{(1)}-\lambda^{(3)})}{\lambda^{(3)}}C_2 e^{-\lambda^{(3)}x} + (\gamma-1)p_1'(x), \tag{68}$$

where

$$\begin{aligned}p_1'(x) \;=\; & \frac{M^2}{(\gamma M^2-1)}\left\{\frac{1}{(1-x)}\left[\frac{\alpha_1 e^{\lambda^{(2)}(1-x)}}{(\lambda^{(2)}-\lambda^{(1)})} + \frac{\alpha_2 e^{\lambda^{(3)}(1-x)}}{(\lambda^{(3)}-\lambda^{(1)})} + A_4 e^{\lambda^{(1)}(1-x)}\right]\right. \\ & + \ln(1-x)\left[\alpha_1\frac{(\lambda^{(2)}-\lambda^{(1)})}{(\lambda^{(2)}-\lambda^{(3)})}e^{\lambda^{(2)}(1-x)} - \alpha_2\frac{(\lambda^{(3)}-\lambda^{(1)})}{(\lambda^{(2)}-\lambda^{(3)})}e^{\lambda^{(3)}(1-x)}\right] \\ & + e^{\lambda^{(3)}(1-x)}\mathrm{Ei}_1[(\lambda^{(3)}-\lambda^{(2)})(1-x)]\frac{\alpha_1(\lambda^{(3)}-\lambda^{(1)})^2}{(\lambda^{(2)}-\lambda^{(3)})(\lambda^{(2)}-\lambda^{(1)})} \\ & - e^{\lambda^{(2)}(1-x)}\mathrm{Ei}_1[(\lambda^{(2)}-\lambda^{(3)})(1-x)]\frac{\alpha_2(\lambda^{(2)}-\lambda^{(1)})^2}{(\lambda^{(2)}-\lambda^{(3)})(\lambda^{(3)}-\lambda^{(1)})} \\ & - e^{\lambda^{(2)}(1-x)}\mathrm{Ei}_1[(\lambda^{(2)}-\lambda^{(1)})(1-x)]A_4\frac{(\lambda^{(2)}-\lambda^{(1)})^2}{(\lambda^{(2)}-\lambda^{(3)})} \\ & \left. + e^{\lambda^{(3)}(1-x)}\mathrm{Ei}_1[(\lambda^{(3)}-\lambda^{(1)})(1-x)]A_4\frac{(\lambda^{(3)}-\lambda^{(1)})^2}{(\lambda^{(2)}-\lambda^{(3)})}\right\},\end{aligned} \tag{69}$$

and $\mathrm{Ei}_1(\zeta)$ is the complex exponential integral

$$\mathrm{Ei}_1(\zeta) = \int_\zeta^\infty \frac{e^{-t}}{t}\,\mathrm{dt}, \quad |\arg\,\zeta| < \pi. \tag{70}$$

Also, C_1 and C_2 are constants which are determined below from the shock conditions (34). From (66), the transverse velocity perturbation v' is given by

$$v'(x) = -\frac{ik}{\lambda^{(2)}} C_1 e^{-\lambda^{(2)}x} - \frac{ik}{\lambda^{(3)}} C_2 e^{-\lambda^{(3)}x} + C_3 e^{-\lambda^{(1)}x} - ik(\gamma-1)v_1'(x), \tag{71}$$

where

$$\begin{aligned} v_1'(x) \;=\; & \frac{M_s}{(\gamma M_s^2 - 1)} \times \\ & \left\{ -\ln(1-x) \left[\frac{\alpha_1}{(\lambda^{(2)} - \lambda^{(3)})} e^{\lambda^{(2)}(1-x)} - \frac{\alpha_2}{(\lambda^{(2)} - \lambda^{(3)})} e^{\lambda^{(3)}(1-x)} \right] \right. \\ & -e^{\lambda^{(3)}(1-x)} \mathrm{Ei}_1[(\lambda^{(3)} - \lambda^{(2)})(1-x)] \frac{\alpha_1(\lambda^{(3)} - \lambda^{(1)})}{(\lambda^{(2)} - \lambda^{(3)})(\lambda^{(2)} - \lambda^{(1)})} \\ & +e^{\lambda^{(2)}(1-x)} \mathrm{Ei}_1[(\lambda^{(2)} - \lambda^{(3)})(1-x)] \frac{\alpha_2(\lambda^{(2)} - \lambda^{(1)})}{(\lambda^{(2)} - \lambda^{(3)})(\lambda^{(3)} - \lambda^{(1)})} \\ & +e^{\lambda^{(2)}(1-x)} \mathrm{Ei}_1[(\lambda^{(2)} - \lambda^{(1)})(1-x)] \frac{A_4(\lambda^{(2)} - \lambda^{(1)})}{(\lambda^{(2)} - \lambda^{(3)})} \\ & \left. -e^{\lambda^{(3)}(1-x)} \mathrm{Ei}_1[(\lambda^{(3)} - \lambda^{(1)})(1-x)] \frac{A_4(\lambda^{(3)} - \lambda^{(1)})}{(\lambda^{(2)} - \lambda^{(3)})} \right\}. \end{aligned} \tag{72}$$

Form (65), the horizontal perturbation $u'(x)$ is given by

$$u'(x) = C_1 e^{-\lambda^{(2)}x} + C_2 e^{-\lambda^{(3)}x} + \frac{ik}{\lambda^{(1)}} C_3 e^{-\lambda^{(1)}x} + (\gamma-1)u_1'(x), \tag{73}$$

where

$$\begin{aligned} u_1'(x) \;=\; & \frac{M_s}{(\gamma M_s^2 - 1)} \times \\ & \left\{ -\frac{1}{(1-x)} \left[\frac{\alpha_1 e^{\lambda^{(2)}(1-x)}}{(\lambda^{(2)} - \lambda^{(1)})} + \frac{\alpha_2 e^{\lambda^{(3)}(1-x)}}{(\lambda^{(3)} - \lambda^{(1)})} + A_4 e^{\lambda^{(1)}(1-x)} \right] \right. \\ & +\ln(1-x) \left[-\frac{\alpha_1 \lambda^{(2)}}{(\lambda^{(2)} - \lambda^{(3)})} e^{\lambda^{(2)}(1-x)} + \frac{\alpha_2 \lambda^{(3)}}{(\lambda^{(2)} - \lambda^{(3)})} e^{\lambda^{(3)}(1-x)} \right] \\ & -e^{\lambda^{(3)}(1-x)} \mathrm{Ei}_1[(\lambda^{(3)} - \lambda^{(2)})(1-x)] \frac{\alpha_1 \lambda^{(3)}(\lambda^{(3)} - \lambda^{(1)})}{(\lambda^{(2)} - \lambda^{(3)})(\lambda^{(2)} - \lambda^{(1)})} \\ & +e^{\lambda^{(2)}(1-x)} \mathrm{Ei}_1[(\lambda^{(2)} - \lambda^{(3)})(1-x)] \frac{\alpha_2 \lambda^{(2)}(\lambda^{(2)} - \lambda^{(1)})}{(\lambda^{(2)} - \lambda^{(3)})(\lambda^{(3)} - \lambda^{(1)})} \\ & +e^{\lambda^{(2)}(1-x)} \mathrm{Ei}_1[(\lambda^{(2)} - \lambda^{(1)})(1-x)] \frac{A_4 \lambda^{(2)}(\lambda^{(2)} - \lambda^{(1)})}{(\lambda^{(2)} - \lambda^{(3)})} \\ & \left. -e^{\lambda^{(3)}(1-x)} \mathrm{Ei}_1[(\lambda^{(3)} - \lambda^{(1)})(1-x)] \frac{A_4 \lambda^{(3)}(\lambda^{(3)} - \lambda^{(1)})}{(\lambda^{(2)} - \lambda^{(3)})} \right\}. \end{aligned} \tag{74}$$

The density perturbation $\rho'(x)$ is given by the last of equations (40),

$$\rho' = \gamma p' - T', \tag{75}$$

where $p'(x)$ is given by (68) and $T'(x)$ is given by (59). Finally, the coefficients C_1, C_2 and C_3 are determined from the shock conditions (34) by

$$\begin{aligned}
C_1 &= \left[\left(\frac{\lambda^{(1)}-\lambda^{(3)}}{\lambda^{(3)}}\right)(u'(0)-(\gamma-1)u_1'(0)-\frac{ik}{\lambda^{(1)}}(v'(0)+ik(\gamma-1)v_1'(0)))\right. \\
&\quad \left.-\frac{1}{M_s}\left(1-\frac{k^2}{\lambda^{(1)}\lambda^{(3)}}\right)(p'(0)-(\gamma-1)p_1'(0))\right] \Big/ \\
&\quad \left[\left(1-\frac{k^2}{\lambda^{(1)}\lambda^{(2)}}\right)\left(\frac{\lambda^{(1)}-\lambda^{(3)}}{\lambda^{(3)}}\right)-\left(1-\frac{k^2}{\lambda^{(1)}\lambda^{(3)}}\right)\left(\frac{\lambda^{(1)}-\lambda^{(2)}}{\lambda^{(2)}}\right)\right] \\
C_2 &= \left[\left(\frac{\lambda^{(1)}-\lambda^{(2)}}{\lambda^{(2)}}\right)(u'(0)-(\gamma-1)u_1'(0)-\frac{ik}{\lambda^{(1)}}(v'(0)+ik(\gamma-1)v_1'(0)))\right. \\
&\quad \left.-\frac{1}{M_s}\left(1-\frac{k^2}{\lambda^{(1)}\lambda^{(2)}}\right)(p'(0)-(\gamma-1)p_1'(0))\right] \Big/ \\
&\quad \left[\left(1-\frac{k^2}{\lambda^{(1)}\lambda^{(3)}}\right)\left(\frac{\lambda^{(1)}-\lambda^{(2)}}{\lambda^{(2)}}\right)-\left(1-\frac{k^2}{\lambda^{(1)}\lambda^{(2)}}\right)\left(\frac{\lambda^{(1)}-\lambda^{(3)}}{\lambda^{(3)}}\right)\right] \\
C_3 &= v'(0)+ik(\gamma-1)v_1'(0)+\frac{ikC_1}{\lambda^{(2)}}+\frac{ikC_2}{\lambda^{(3)}}
\end{aligned} \tag{76}$$

Thus through the formal use of the Newtonian limit where $\gamma \to 1$, we have succeeded in deriving an asymptotic solution to the eigenfunction structure equations in the induction zone of a detonation wave. We can now describe the essential mechanisms for the generation of hydrodynamic instabilities in the IZ. For a given shock perturbation and to leading order in the Newtonian limit, acoustic pressure changes propagate this change around the induction zone independently of any perturbation in the chemical reaction rate. The leading-order acoustic perturbation behaviour at the fire zone is determined by a matching problem across the fire into the equilibrium (or burnt) zone where an acoustic radiation condition is employed. Details of this are given below. Subsequently, this pressure wave propagation, which occurs along the paths corresponding to $\lambda^{(2)}$ and $\lambda^{(3)}$, interact with changes of $O(\gamma-1)$ in the temperature perturbation at the shock. The latter are propagated along the particle paths corresponding to $\lambda^{(1)}$ and in combination with the leading-order acoustic changes, generate a change in the IZ temperature perturbation at $O(\gamma-1)$. This will lead to a shift in the fire zone position, which again is explored in detail below. However, the shift will modify the nature of the pressure disturbance behaviour both at the fire front and in the burnt zone, and thus affect the leading-order, chemically uninfluenced pressure wave propagation in the IZ, thereby establishing a feedback cycle between acoustic wave propagation and entropy changes. If this feedback cycle is sufficently strong, the detonation will become linearly unstable. The temperature perturbation at $O(\gamma-1)$ also leads to a spatially non-uniform perturbation in the reaction rate at $O(\gamma-1)$ which then forces $O(\gamma-1)$ changes

in the reactant mass fraction and $O(\gamma-1)$ changes in the pressure and velocity perturbations. Thus, we conclude that the mechanism of detonation instability is generated by this intricate acoustic-thermal interaction.

In order to determine the response of the fire zone to the presence of the perturbations, required to describe the round-trip traversal of acoustic waves in the IZ between the fire and shock, the shift in flame position corresponding to a linearized perturbation and the resulting behaviour in the burnt gas must now be calculated. It will be shown that near the fire, the induction zone perturbation solutions possess a simple pole singularity, which render the expansions (28) non-uniform. It is then necessary to employ a Lighthill straining of the induction zone co-ordinate in order to remove the non-uniformity, and to be able to match the IZ solution to the fire zone solution. As a result of this singular perturbation analysis, we can explicitly calculate the analytical response of the fire zone position to the linear perturbations in the IZ.

4(d) Fire zone displacement

In order to determine the fire zone displacement which occurs due to the presence of the linearized perturbations, the behaviour of the IZ eigenfunction expansions (59), (61), (68), (71) and (73) need to be determined at the end of the induction zone. As $x \to 1$, the temperature perturbation (59) has the expansion,

$$T' = (\gamma-1)\left[\frac{\alpha}{1-x}\right] + T'_F + \cdots, \tag{77}$$

where

$$T'_F = (\gamma-1)\left[\frac{\alpha_1\lambda^{(2)}}{(\lambda^{(2)}-\lambda^{(1)})} + \frac{\alpha_2\lambda^{(3)}}{(\lambda^{(3)}-\lambda^{(1)})} + A_4\lambda^{(1)} - \alpha_1 - \alpha_2\right], \tag{78}$$

and

$$\alpha = \frac{\alpha_1}{(\lambda^{(2)}-\lambda^{(1)})} + \frac{\alpha_2}{(\lambda^{(3)}-\lambda^{(1)})} + A_4. \tag{79}$$

Thus as $x \to 1$, the temperature perturbation possess a simple pole singularity. The reactant mass perturbation (61) behaviour as $x \to 1$ is given by,

$$Y' = -(\gamma-1)\frac{(M_s^2-1)}{\beta(\gamma M_s^2-1)}\left[\frac{\alpha}{(1-x)}\right] + Y'_F + \cdots, \tag{80}$$

where

$$Y'_F = (\gamma-1)\left[-\frac{(M_s^2-1)}{\beta(\gamma M_s^2-1)}\left[\frac{\alpha_1\lambda^{(2)}}{(\lambda^{(2)}-\lambda^{(1)})} + \frac{\alpha_2\lambda^{(3)}}{(\lambda^{(3)}-\lambda^{(1)})} + A_4\lambda^{(1)}\right] + A_5 e^{-\lambda^{(1)}}\right], \tag{81}$$

which also possess a simple pole singularity at $x = 1$. Since the exponential integral has the expansion

$$\mathrm{Ei}_1(\omega(1-x)) = -\gamma^* - \ln(1-x) - \ln\omega + O(1-x), \tag{82}$$

as $x \to 1^-$, where γ^* is Euler's constant,

$$\gamma^* = \lim_{n\to\infty}(\sum_{i=1}^{n} 1/i - \ln(n)) = 0.5772156649, \tag{83}$$

the pressure perturbation behaviour (68) as $x \to 1$ is given by

$$p' = (\gamma-1)\frac{M_s^2}{(\gamma M_s^2-1)}\left[\frac{\alpha}{(1-x)} + p'_{\ln}\ln(1-x)\right] + p'_F + \cdots, \tag{84}$$

where

$$p'_{\ln} = \alpha(\lambda^{(2)} + \lambda^{(3)} - 2\lambda^{(1)}), \tag{85}$$

and

$$\begin{aligned} p'_F \;=\; & M_s\frac{(\lambda^{(1)}-\lambda^{(2)})}{\lambda^{(2)}}C_1e^{-\lambda^{(2)}} + M_s\frac{(\lambda^{(1)}-\lambda^{(3)})}{\lambda^{(3)}}C_2e^{-\lambda^{(3)}} \\ & +(\gamma-1)\frac{M_s^2}{(\gamma M_s^2-1)}\times\left\{\left[\frac{\alpha_1\lambda^{(2)}}{(\lambda^{(2)}-\lambda^{(1)})} + \frac{\alpha_2\lambda^{(3)}}{(\lambda^{(3)}-\lambda^{(1)})} + A_4\lambda^{(1)}\right]\right. \\ & -\left[\gamma^* + \ln(\lambda^{(3)}-\lambda^{(2)})\right]\alpha_1\frac{(\lambda^{(3)}-\lambda^{(1)})^2}{(\lambda^{(2)}-\lambda^{(3)})(\lambda^{(2)}-\lambda^{(1)})} \\ & +\left[\gamma^* + \ln(\lambda^{(2)}-\lambda^{(3)})\right]\alpha_2\frac{(\lambda^{(2)}-\lambda^{(1)})^2}{(\lambda^{(2)}-\lambda^{(3)})(\lambda^{(3)}-\lambda^{(1)})} \\ & \left.+\left[\gamma^* + \ln(\lambda^{(2)}-\lambda^{(1)})\right]A_4\frac{(\lambda^{(2)}-\lambda^{(1)})^2}{(\lambda^{(2)}-\lambda^{(3)})} - \left[\gamma^* + \ln(\lambda^{(3)}-\lambda^{(1)})\right]A_4\frac{(\lambda^{(3)}-\lambda^{(1)})^2}{(\lambda^{(2)}-\lambda^{(3)})}\right\}. \end{aligned} \tag{86}$$

The horizontal velocity perturbation $u'(x)$ (73) as $x \to 1$ becomes,

$$u'(x) = -(\gamma-1)\frac{M_s}{(\gamma M_s^2-1)}\left[\frac{\alpha}{(1-x)} + u'_{\ln}\ln(1-x)\right] + u'_F + \cdots, \tag{87}$$

where

$$u'_{\ln} = \alpha(\lambda^{(3)} + \lambda^{(2)} - \lambda^{(1)}), \tag{88}$$

and

$$
\begin{aligned}
u'_F &= C_1 e^{-\lambda^{(2)}} + C_2 e^{-\lambda^{(3)}} + \frac{ik}{\lambda^{(1)}} C_3 e^{-\lambda^{(1)}} \\
&+(\gamma-1)\frac{M_s}{(\gamma M_s^2-1)} \times \left\{ -\left[\frac{\alpha_1 \lambda^{(2)}}{(\lambda^{(2)}-\lambda^{(1)})} + \frac{\alpha_2 \lambda^{(3)}}{(\lambda^{(3)}-\lambda^{(1)})} + A_4 \lambda^{(1)} \right] \right. \\
&+(\gamma^* + \ln(\lambda^{(3)}-\lambda^{(2)}))\frac{\alpha_1 \lambda^{(3)}(\lambda^{(3)}-\lambda^{(1)})}{(\lambda^{(2)}-\lambda^{(3)})(\lambda^{(2)}-\lambda^{(1)})} \\
&-(\gamma^* + \ln(\lambda^{(2)}-\lambda^{(3)}))\frac{\alpha_2 \lambda^{(2)}(\lambda^{(2)}-\lambda^{(1)})}{(\lambda^{(2)}-\lambda^{(3)})(\lambda^{(3)}-\lambda^{(1)})} \\
&-(\gamma^* + \ln(\lambda^{(2)}-\lambda^{(1)}))\frac{A_4 \lambda^{(2)}(\lambda^{(2)}-\lambda^{(1)})}{(\lambda^{(2)}-\lambda^{(3)})} \\
&\left. +(\gamma^* + \ln(\lambda^{(3)}-\lambda^{(1)}))\frac{A_4 \lambda^{(3)}(\lambda^{(3)}-\lambda^{(1)})}{(\lambda^{(2)}-\lambda^{(3)})} \right\}.
\end{aligned}
\tag{89}
$$

The transverse velocity component $v'(x)$ (71) as $x \to 1$ is given by

$$
v'(x) = -ik(\gamma-1)\frac{M_s}{(\gamma M_s^2-1)} v'_{\ln} \ln(1-x) + v'_F + \cdots, \tag{90}
$$

where,

$$
v'_{\ln} = -\alpha, \tag{91}
$$

and

$$
\begin{aligned}
v'_F &= -\frac{ik}{\lambda^{(2)}} C_1 e^{-\lambda^{(2)}} - \frac{ik}{\lambda^{(3)}} C_2 e^{-\lambda^{(3)}} + C_3 e^{-\lambda^{(1)}} \\
&-ik(\gamma-1)\frac{M_s}{(\gamma M_s^2-1)} \times \left\{ (\gamma^* + \ln(\lambda^{(3)}-\lambda^{(2)}))\frac{\alpha_1(\lambda^{(3)}-\lambda^{(1)})}{(\lambda^{(2)}-\lambda^{(3)})(\lambda^{(2)}-\lambda^{(1)})} \right. \\
&-(\gamma^* + \ln(\lambda^{(2)}-\lambda^{(3)}))\frac{\alpha_2(\lambda^{(2)}-\lambda^{(1)})}{(\lambda^{(2)}-\lambda^{(3)})(\lambda^{(3)}-\lambda^{(1)})} \\
&-(\gamma^* + \ln(\lambda^{(2)}-\lambda^{(1)}))\frac{A_4(\lambda^{(2)}-\lambda^{(1)})}{(\lambda^{(2)}-\lambda^{(3)})} \\
&\left. +(\gamma^* + \ln(\lambda^{(3)}-\lambda^{(1)}))\frac{A_4(\lambda^{(3)}-\lambda^{(1)})}{(\lambda^{(2)}-\lambda^{(3)})} \right\}.
\end{aligned}
\tag{92}
$$

Finally, the density perturbation $\rho'(x)$ as $x \to 1$ is given by

$$
\rho' = (\gamma-1)\frac{1}{(\gamma M^2-1)}\frac{\alpha}{(1-x)} + \frac{\gamma(\gamma-1)M^2}{(\gamma M^2-1)} p'_{\ln} \ln(1-x) + \rho'_F + \cdots, \tag{93}
$$

where

$$
\rho'_F = \gamma p'_F - T'_F. \tag{94}
$$

In order to understand the role of the simple pole singularity which appears in each of the expansions (77), (80), (84), (87), (90) and (93) these expansions can be combined with (20) and (28) and written as,

$$
\begin{aligned}
T &\sim 1 - \frac{1}{\theta}\ln(1-x) + (\gamma-1)\frac{\alpha}{(1-x)}e^{iky}e^{\lambda t} + T'_F e^{iky}e^{\lambda t} + \cdots, \\
Y &\sim 1 + \frac{(M_s^2-1)}{\beta(\gamma M_s^2-1)}\left[\frac{1}{\theta}\ln(1-x) - (\gamma-1)\left[\frac{\alpha}{(1-x)} + Y'_{\ln}\ln(1-x)\right]e^{iky}e^{\lambda t}\right] \\
&\qquad + Y'_F e^{iky}e^{\lambda t} + \cdots, \\
p &\sim 1 - \frac{M_s^2}{(\gamma M_s^2-1)}\left[\frac{1}{\theta}\ln(1-x) - (\gamma-1)\left[\frac{\alpha}{(1-x)} + p'_{\ln}\ln(1-x)\right]e^{iky}e^{\lambda t}\right] \\
&\qquad + p'_F e^{iky}e^{\lambda t} + \cdots, \\
u &\sim M_s + \frac{M_s}{(\gamma M_s^2-1)}\left[\frac{1}{\theta}\ln(1-x) - (\gamma-1)\left[\frac{\alpha}{(1-x)} + u'_{\ln}\ln(1-x)\right]e^{iky}e^{\lambda t}\right] \\
&\qquad + u'_F e^{iky}e^{\lambda t} + \cdots, \\
v &\sim -\frac{ikM_s}{(\gamma M_s^2-1)}(\gamma-1)v'_{\ln}\ln(1-x)e^{iky}e^{\lambda t} + v'_F e^{iky}e^{\lambda t} + \cdots, \\
\rho &\sim 1 - \frac{1}{(\gamma M_s^2-1)}\left[\frac{1}{\theta}\ln(1-x) - (\gamma-1)\left[\frac{\alpha}{(1-x)} + \gamma(\gamma-1)M_s^2 p'_{\ln}\ln(1-x)\right]e^{iky}e^{\lambda t}\right] \\
&\qquad + \rho'_F e^{iky}e^{\lambda t} + \cdots.
\end{aligned}
\tag{95}
$$

Thus the presence of the pole singularity as $x \to 1$ in the perturbation quantities introduces a non-uniformity in the expansions (95) near the fire front. Essentially, the non-uniformity develops due to the failure to account for perturbations in the fire front position that are generated by the small unsteady perturbations in the induction zone. The non-uniformity can be removed by straining the location of the fire front by a simple application of Lighthill's method of strained co-ordinates. Also, it can be verified that an analysis of the perturbed structure of the fire zone region necessitates that matching to the IZ solution requires a leading-order match to a logarithmic type solution, in the standard way. This can be achieved through the Lighthill

straining applied to equations (95). After doing so, equations (95) then take the regular form,

$$
\begin{aligned}
T &\sim 1 - \frac{1}{\theta}\ln(F(y,t)-x) + T'_F e^{iky}e^{\lambda t} + \cdots,\\
Y &\sim 1 + \frac{(M_s^2-1)}{\theta\beta(\gamma M^2-1)}\left[1-\theta(\gamma-1)Y'_{\ln}e^{iky}e^{\lambda t}\right]\ln(F(y,t)-x) + Y'_F e^{iky}e^{\lambda t} + \cdots,\\
p &\sim 1 - \frac{M_s^2}{\theta(\gamma M_s^2-1)}\left[1-\theta(\gamma-1)p'_{\ln}e^{iky}e^{\lambda t}\right]\ln(F(y,t)-x) + p'_F e^{iky}e^{\lambda t} + \cdots,\\
u &\sim M_s + \frac{M_s}{\theta(\gamma M_s^2-1)}\left[1-\theta(\gamma-1)u'_{\ln}e^{iky}e^{\lambda t}\right]\ln(F(y,t)-x) + u'_F e^{iky}e^{\lambda t} + \cdots,\\
v &\sim -\frac{ikM_s}{(\gamma M_s^2-1)}(\gamma-1)v'_{\ln}e^{iky}e^{\lambda t}\ln(F(y,t)-x) + v'_F e^{iky}e^{\lambda t} + \cdots,\\
\rho &\sim 1 - \frac{1}{\theta(\gamma M_s^2-1)}\left[1-\theta\gamma(\gamma-1)M^2 p'_{\ln}e^{iky}e^{\lambda t}\right]\ln(F(y,t)-x) + \rho'_F e^{iky}e^{\lambda t} + \cdots,
\end{aligned}
\tag{96}
$$

where

$$x = F(y,t) = 1 - \theta(\gamma-1)\alpha e^{iky}e^{\lambda t}, \tag{97}$$

gives the perturbation in the position of the fire about $x = 1$, corresponding to the present of the perturbations in the induction zone. Thus in order to remove the non-uniformity in expansions (95), the position of the fire has be shifted by an amount $O(\alpha(\gamma-1)\theta)$. We also note that relative to the steady shock co-ordinate system, n, the perturbation in fire position about the steady fire zone location $n = 1$ is given by

$$n = 1 + f' e^{iky}e^{\lambda t}, \tag{98}$$

where,

$$f' = h' - \theta(\gamma-1)\alpha. \tag{99}$$

We are now in a position to complete the analysis, first by calculating the behaviour of the linearized perturbations in the burnt zone and then matching this behaviour to the expansions (96) across the fire.

4(e) Burnt zone perturbations.

With reference to Fig. 1, in the limit of large activation energy an exponentially small fire region and exponentially small relaxation region connect the induction zone to the burnt zone (BZ) in which reaction has effectively terminated, i.e. where

$$Y = \text{e.s.t.} \quad \text{as} \quad \theta \to \infty. \tag{100}$$

The linear perturbations to the steady state in the burnt zone are determined by an expansion in the normal mode form,

$$\mathbf{z} = \mathbf{z}_b^* + \mathbf{z}'_b(x)e^{\lambda t}e^{iky}, \tag{101}$$

where the subscript b is used to denote burnt zone quantities. Substituting expansions (101) into (11) with $Y = 0$, the pressure and velocity perturbation eigenfunctions in the BZ are determined by the standard two-dimensional linear acoustic equations,

$$\begin{aligned}
&\lambda u_b' + M_b \nu_b \frac{du_b'}{dx} + \frac{1}{\mu_b}\frac{dp_b'}{dx} = 0, \\
&\lambda v_b' + M_b \nu_b \frac{dv_b'}{dx} + \frac{ik}{\mu_b} p_b' = 0, \\
&\lambda p_b' + M_b \nu_b \frac{dp_b'}{dx} + \nu_b^2 \mu_b \left(\frac{du_b'}{dx} + ikv_b'\right) = 0,
\end{aligned} \tag{102}$$

where M_b, μ_b and ν_b are given by,

$$M_b = \frac{\tilde{u}_b^*}{\tilde{c}_b^*}, \quad \mu_b = \frac{\tilde{\rho}_b^*}{\tilde{\rho}_s^*}, \quad \nu_b = \frac{\tilde{c}_b^*}{\tilde{c}_s^*}, \tag{103}$$

and represent the Mach number of the steady flow in the BZ, the ratio of the unperturbed material density in the BZ to that at the detonation shock and the ratio of the unperturbed adiabatic sound speed in the BZ to that at the detonation shock respectively. The two velocity perturbations u_b' and v_b' can be eliminated from (102) to give the second order linear equation for p_b',

$$(M_b^2 - 1)\nu_b \frac{d^2 p_b'}{dx^2} + 2\lambda M_b \frac{dp_b'}{dx} + \nu_b \left(k^2 + \frac{\lambda^2}{\nu_b^2}\right) p_b' = 0. \tag{104}$$

For $M_b < 1$, i.e. when the detonation is overdriven and the flow in the BZ is subsonic, the characteristic roots of equation (104) are given by

$$\lambda_b^{(2,3)} = -\frac{1}{\nu_b(M_b^2 - 1)}\left[M_b\lambda \pm \sqrt{\lambda^2 + k^2\nu_b^2(1 - M_b^2)}\right], \tag{105}$$

and correspond to the surfaces of acoustic wave propagation in the BZ. The root $\lambda_b^{(2)}$ represents upstream propagation from infinity to the rear of the fire, while the root $\lambda_b^{(3)}$ represents downstream propagation from the fire. On the other hand, for $M_b = 1$, i.e. when the steady detonation is travelling at the CJ velocity and the flow in the BZ is exactly sonic, the linear equation (104) is degenerate and one of the characteristic roots in (105) is eliminated. The remaining characteristic root is given by

$$\lambda_b^{(4)} = -\frac{\nu_b}{2\lambda}\left(k^2 + \frac{\lambda^2}{\nu_b^2}\right), \tag{106}$$

which corresponds to downstream propagation from the fire. The fact that the upstream root is eliminated is due to the particular nature of the sonic flow. Due to the presence of the sonic point at the end of the fire zone, the burnt zone and detonation wave are acoustically decoupled and perturbations originating upstream are unable to penetrate into the detonation structure. This has significant implications for the determination of a compatibility condition in the linear

stability analysis, as will be discussed below. For $M_b < 1$, the general solution to (104) is given by,

$$\begin{aligned} p_b' &= A_{1b}e^{\lambda_b^{(2)}x} + A_{2b}e^{\lambda_b^{(3)}x}, \\ u_b' &= -\frac{ikA_{3b}}{\lambda_b^{(1)}}e^{\lambda_b^{(1)}x} - \frac{\lambda_b^{(2)}A_{1b}e^{\lambda_b^{(2)}x}}{M_b\mu_b\nu_b(\lambda_b^{(2)}-\lambda_b^{(1)})} - \frac{\lambda_b^{(3)}A_{2b}e^{\lambda_b^{(3)}x}}{M_b\mu_b\nu_b(\lambda_b^{(3)}-\lambda_b^{(1)})}, \\ v_b' &= A_{3b}e^{\lambda_b^{(1)}x} - \frac{ikA_{1b}e^{\lambda_b^{(2)}x}}{M_b\mu_b\nu_b(\lambda_b^{(2)}-\lambda_b^{(1)})} - \frac{ikA_{2b}e^{\lambda_b^{(3)}x}}{M_b\mu_b\nu_b(\lambda_b^{(3)}-\lambda_b^{(1)})}, \end{aligned} \tag{107}$$

for constants A_{1b}, A_{2b}, A_{3b}, where

$$\lambda_b^{(1)} = -\frac{\lambda}{M_b\nu_b}, \tag{108}$$

corresponds to vorticity and entropy wave propagation in the burnt zone. When $M_b = 1$, the general solution to (104) is given by

$$\begin{aligned} p_b' &= A_{4b}e^{\lambda_b^{(4)}x}, \\ u_b' &= -\frac{ikA_{5b}}{\lambda_b^{(5)}}e^{\lambda_b^{(5)}x} - \frac{\lambda_b^{(4)}A_{4b}e^{\lambda_b^{(4)}x}}{\mu_b\nu_b(\lambda_b^{(4)}-\lambda_b^{(5)})}, \\ v_b' &= A_{5b}e^{\lambda_b^{(5)}x} - \frac{ikA_{4b}e^{\lambda_b^{(4)}x}}{\mu_b\nu_b(\lambda_b^{(4)}-\lambda_b^{(5)})}, \end{aligned} \tag{109}$$

for constants A_{4b}, A_{5b}, where

$$\lambda_b^{(5)} = -\frac{\lambda}{\nu_b}, \tag{110}$$

also corresponds to vorticity and entropy wave propagation in the BZ, but when $M_b = 1$.

4(f) Radiation condition for overdriven detonation waves.

For overdriven detonation waves when $M_b < 1$, an additional condition on the perturbations in the BZ zone is required. We employ a standard acoustic radiation condition in the BZ in which the root $\lambda_b^{(2)}$, which represents upstream propagation from infinity, is eliminated. Therefore we set,

$$A_{1b} = 0, \tag{111}$$

and from equations (107), this leads directly to the compatibility relation,

$$\lambda u_b' - ikM_b\nu_b v_b' - \frac{p_b'}{\mu_b\nu_b}\left[\lambda^2 + k^2\nu_b^2(1-M_b^2)\right]^{1/2} = 0, \tag{112}$$

for perturbations in the BZ. For one-dimensional disturbances, i.e when $k = 0$, the compatibility relation (112) reduces to,

$$u_b' = \frac{p_b'}{\nu_b\mu_b}. \tag{113}$$

It should be noted that for overdriven detonation waves, the relation (112) is not unique in determining a condition on the behaviour of perturbations in the burnt gas. One could, for example, easily impose a piston type condition where the velocity perturbation far downstream of the detonation is zero.

4(g) Radiation condition for CJ detonation waves.

When $M_b = 1$, the sonic condition eliminates the upstream propagating acoustic waves. The three equations (109) then comprise of the two unknown constants A_{4b} and A_{5b}. Thus for a regular solution, the equations (109) must necessarily satisfy the compatibility relation

$$\lambda u_b' - ik\nu_b v_b' - \frac{\lambda p_b'}{\mu_b \nu_b} = 0. \tag{114}$$

We note that this is simply the limiting form of the acoustic radiation condition (112) for overdriven detonation waves when $M_b \to 1^-$. However, unlike the situation for the overdriven detonation, the CJ detonation *must* necessarily satisfy the condition (114) in the burnt zone, and there is no arbitrariness in the specification of a compatibility condition. As such, it will be demonstrated below that we must then impose a further compatibility condition on the jump relations across the fire zone for the CJ detonation in order to complete the specification of the linear stability problem.

4(h) Rankine-Hugoniot deflagration relations across the discontinuous fire zone

Having determined the behaviour of the linear perturbation quantities in the burnt zone and induction zone of the detonation, we are now required to match these quantities across the fire and relaxation zones. In the limit of high activation energy these zones are exponentially small, so that, providing the wavelength of the disturbance is sufficiently long, the fire and relaxation zones can be treated as a standard Rankine-Hugoniot discontinuity (Buckmaster 1989). For high-frequency disturbances, the structure of the flame zone must be accounted for in the linear stability analysis. This analysis is not treated here. For the present paper, we limit our attention to wavelengths that are much longer than the flame thickness. In general, it is easy to demonstrate that by substituting the BZ expansions (101) and the IZ expansions (96) into the Rankine-Hugoniot deflagration relations across the perturbed fire zone given by (98), leads to the equations,

$$\begin{aligned}
\mu_b(u_b' - \lambda f') + M_b\nu_b\rho_b' &= (u_F' - \lambda f') + M\rho_F', \\
p_b' + \mu_b\nu_b M_b(2u_b' - \lambda f') + \nu_b^2 M_b^2 \rho_b' &= p_F' + M(2u_F' - \lambda f') + M^2\rho_F', \\
(\frac{\gamma}{\mu_b}p_b' - \frac{\nu_b^2}{\mu_b}\rho_b') + (\gamma - 1)M_b\nu_b(u_b' - \lambda f') &= \beta Y_F' + (\gamma p_F' - \rho_F') + (\gamma - 1)M(u_F' - \lambda f'), \\
ik\nu_b M_b f' + v_b' &= ikMf' + v_F',
\end{aligned} \tag{115}$$

which relate the induction quantities $\mathbf{z}'_F$ evaluated at the fire to the burnt perturbations $\mathbf{z}'_b$. The first three of these relations can be put into matrix form as

$$\mathbf{A}_b \cdot \zeta'_b = \begin{bmatrix} M \\ M^2 \\ -1 \end{bmatrix} \rho'_F + \begin{bmatrix} 1 \\ 2M \\ (\gamma-1)M \end{bmatrix} u'_F + \begin{bmatrix} 0 \\ 1 \\ \gamma \end{bmatrix} p'_F + \begin{bmatrix} 0 \\ 0 \\ \beta \end{bmatrix} Y'_F + \begin{bmatrix} \mu_b - 1 \\ 0 \\ (\gamma-1)(M_b\nu_b - M) \end{bmatrix} \lambda f', \tag{116}$$

where

$$\zeta'_b = [\rho'_b,\ u'_b,\ p'_b]^{\mathrm{T}} \quad \text{and} \quad \mathbf{A}_b = \begin{bmatrix} M_b\nu_b & \mu_b & 0 \\ \nu_b^2 M_b^2 & 2\mu_b\nu_b M_b & 1 \\ -\nu_b^2/\mu_b & (\gamma-1)M_b\nu_b & \gamma/\mu_b \end{bmatrix}. \tag{117}$$

For $M_b < 1$, the matrix $\mathbf{A}_b$ has the inverse,

$$\mathbf{A}_b^{-1} = \frac{1}{(M_b^2-1)} \begin{bmatrix} \dfrac{M_b}{\nu_b}(\gamma+1) & -\dfrac{\gamma}{\nu_b^2} & \dfrac{\mu_b}{\nu_b^2} \\ -\dfrac{\gamma M_b^2+1}{\mu_b} & \dfrac{\gamma M_b}{\mu_b\nu_b} & -\dfrac{M_b}{\nu_b} \\ \nu_b M_b((\gamma-1)M_b^2+2) & -((\gamma-1)M_b^2+1) & M_b^2\mu_b \end{bmatrix}, \tag{118}$$

so that explicit relations for u'_b, p'_b can be written down in terms of f', ρ'_F, u'_F, p'_F and Y'_F as,

$$\begin{aligned} u'_b \;=\; & \lambda f' \left[\frac{1}{(M_b^2-1)} \frac{(\mu_b-1)}{\mu_b} \left[-1 - (1-(\gamma-1)(\mu_b-1))M_b^2 \right] \right] \\ & -\rho'_F \left[\frac{\nu_b M_b}{(M_b^2-1)} \left[-\frac{1}{\nu_b^2} + 1 + ((1-\mu_b) + (\gamma-1)(1-\mu_b))M_b^2 \right] \right] \\ & -u'_F \left[\frac{1}{\mu_b(M_b^2-1)} \left[1 + (1 - 2\mu_b + (\gamma-1)(\mu_b-1)^2)M_b^2 \right] \right] \\ & -p'_F \left[\frac{\gamma}{\mu_b\nu_b} \frac{M_b}{(M_b^2-1)} (\mu_b - 1) \right] \\ & -Y'_F \beta \frac{M_b}{\nu_b(M_b^2-1)}, \end{aligned} \tag{119}$$

and

$$
\begin{aligned}
p'_b &= \lambda f' \left[\frac{\mu_b \nu_b M_b}{(M_b^2 - 1)} \frac{(\mu_b - 1)}{\mu_b} \left[2 - (\gamma - 1)(\mu_b - 1) M_b^2 \right] \right] \\
&+ \rho'_F \left[\frac{\nu_b^2 \mu_b M_b^2}{(M_b^2 - 1)} \left[-\frac{1}{\nu_b^2} + 2 - \mu_b - (\gamma - 1)(\mu_b - 1) M_b^2 \right] \right] \\
&+ u'_F \left[\frac{\nu_b \mu_b M_b}{(M_b^2 - 1)} \frac{(1 - \mu_b)}{\mu_b} \left[2 - (\gamma - 1)(\mu_b - 1) M_b^2 \right] \right] \\
&+ p'_F \left[\frac{1}{(M_b^2 - 1)} \left[-1 + (\mu_b + (\gamma - 1)(\mu_b - 1)) M_b^2 \right] \right] \\
&+ Y'_F \beta \mu_b \frac{M_b^2}{(M_b^2 - 1)},
\end{aligned}
\tag{120}
$$

Form (115), the transverse velocity perturbation v'_b given by

$$
v'_b = ik\nu_b M_b f'(\mu_b - 1) + v'_F. \tag{121}
$$

Then for $M_b < 1$ the dispersion relation is obtained by substituting the jump relations (119)–(121) into the radiation condition (112) and solving for λ using a Newton-Raphson iteration method.

For $M_b = 1$, the matrix $\mathbf{A}_b^{-1}$ is singular. The reason for this is straightforward. In section 4(g) above, it was established that for $M_b = 1$ the burnt perturbations must necessarily satisfy the radiation condition (114) and thus the first three equations in (115) are no longer independent. For $M_b < 1$ these equations are independent and can be inverted. The imposition of the radiation condition (112) is a particular choice which will give a dispersion relation, but it is not unique and other choices, such as the imposition of a piston condition in the BZ could be used for $M_b < 1$. However, for $M_b = 1$ the condition (114) *must* be satisfied. The relation (114) can thus be used to eliminate p'_b from the second of the jump relations (115), whereupon the first and second equations of (115) can be solved for u'_b and ρ'_b to give,

$$
\begin{aligned}
u'_b &= \frac{1}{2\mu_b \nu_b} \left[p'_F + u'_F(2M - \nu_b) + M(M - \nu_b)\rho'_F - \nu_b \lambda f'(\mu_b - 1) \right. \\
&\qquad \left. + \frac{ik}{\lambda} \mu_b \nu_b^2 v'_F + \frac{ik}{\lambda} \mu_b \nu_b^3 (\mu_b - 1) ikf' \right], \\
\rho'_b &= \frac{1}{2\nu_b^2} \left[-p'_F + u'_F(3\nu_b - 2M) + M\rho'_F(3\nu_b - M) + 3\nu_b(\mu_b - 1)\lambda f' \right. \\
&\qquad \left. - \frac{ik}{\lambda} \mu_b \nu_b^2 v'_F - \frac{ik}{\lambda} \mu_b \nu_b^3 (\mu_b - 1) ikf' \right].
\end{aligned}
\tag{122}
$$

Substituting these relationships into the third of equations (115) leads to the following compat-

ibility condition on the Rankine-Hugoniot jump relations for CJ detonation waves, namely

$$\gamma\left(\frac{1}{\mu_b}-1\right)p'_F+\left(\frac{1}{\mu_b}(2\gamma M-\nu_b(\gamma+1))-(\gamma-1)M\right)u'_F+$$
$$\left(\frac{M}{\mu_b}(\gamma M-\nu_b(\gamma+1))+1\right)\rho'_F-\beta Y'_F+\frac{(\mu_b-1)}{\mu_b}\nu_b\left[-(\gamma+1)+(\gamma-1)\mu_b\right]\lambda f'=0. \tag{123}$$

Then for CJ detonation waves the relations for $\mathbf{z}'_F$ are substituted into the compatibility relation (123) which is solved directly to determine for the eigenvalue λ using Newton-Raphson iteration.

5 Dispersion Relation and Linear Stability Spectrum

Below, we present a comparison of the predictions of our asymptotic theory with exact numerical solutions of the linear stability spectrum. Moreover, such comparisons are presented for realistic regimes of the detonation parameters, including those for CJ detonations as well as overdriven detonations.

Figure 2 shows the migration of the real growth rate $\mathrm{Re}(\lambda)$ and frequency $\mathrm{Im}(\lambda)$, calculated from the analytical dispersion relation, as the activation energy E varies for the much studied case of $Q=50$, $f=1.2$ and $\gamma=1.2$. Also shown is the result of a direct numerical solution of the linear disturbance equations (30) for $Q=50$, $f=1.2$ and $\gamma=1.2$ (Short 1996a). Given the previous pathologies associated with the high-activation energy analyses of the detonation linear stability problem, the agreement between the two solutions is excellent. Moreover, the asymptotic theory predicts that the low-frequency root is stable for $E<17.1$, i.e. for sufficiently low activation energies. This compares to a value of $E=30.6$ from the numerical solution. Precisely this behaviour is found in direct numerical simulations of one-dimensional detonation stability problems, where for a sufficiently low activation energy the detonation is predicted to be stable (Quirk 1994). For such activation energies, the feedback cycle between acoustic wave propagation and entropy wave propagation and the resulting perturbations to the fire zone position, as detailed previously, s sufficiently weak as to not generate an instability. As E increases, the asymptotic solution predicts the growth rate to increase, until at $E=42.8$ the oscillatory mode bifurcates into two non-oscillatory modes as previously found numerically by Short (1996a). The numerical value of the bifurcation point is $E=52.8$. Subsequently, the growth rate of one mode increases, while the growth rate of the other non-oscillatory mode decreases. For $E>60$, the asymptotic and numerical solutions for the lower branch are co-incident. For the upper branch, the asymptotic solution remains a good approximation to the numerical solution, even though the growth rates are becoming relatively large.

Figure 3 shows a comparison of the migration of the real growth rate $\mathrm{Re}(\lambda)$ and frequency $\mathrm{Im}(\lambda)$ with activation E of the one-dimensional low-frequency disturbance that is predicted from the asymptotic theory above against a direct numerical solution for the exact spectrum with $Q=50$, $\gamma=1.2$ and $f=1$. Thus as a Chapman-Jouguet detonation wave, the dispersion relation must be obtained from the compatibility condition on the fire-zone jump conditions

(123). Again, the agreement is good. We also remark here that the numerical solutions for the exact spectrum are exceedingly difficult to obtain due to the nature of the sonic condition in CJ waves, and thus we have not calculated exact spectra for values above $E = 60$. Comparatively the same behaviour for the linear stability spectrum is observed in this CJ case as that seen previously in figure 2. The asymptotic dispersion relation predicts that the detonation is stable for a sufficiently low activation activation energy, in this case for $E < 12.4$, compared to a numerical value of $E < 25.3$. Growth rates increase with increasing E and bifurcate into two non-oscillatory modes at $E = 23.9$ (asymptotic solution) and $E = 35.5$ (numerical solution). For $E > 42$, the lower branch of the non-oscillatory mode is co-incident with the numerical solution.

Figure 4 shows a comparison of the much studied case of the migration of the growth rate $\mathrm{Re}(\lambda)$ and frequency $\mathrm{Im}(\lambda)$ with the detonation overdrive f for the one-dimensional low-frequency disturbance predicted from the asymptotic theory above against a direct numerical solution for the exact stability spectrum with $Q = 50$, $\gamma = 1.2$ and $E = 50$. The asymptotic solution mimics precisely the behaviour observed in the numerical solution and predicts stability for $f > 2.34$, compared to a numerical value of $f > 1.73$. This stability boundary and detonation parameter regime has been the source of most of the direct numerical simulations of detonation instability (Fickett and Wood 1966, Bourlioux *et al.* 1991 and Quirk 1994). The asymptotic solution predicts that at $f = 2.34$ a Hopf bifurcation occurs in the low frequency root, rendering the detonation unstable. For decreasing overdrive, the growth rate of this oscillatory mode is predicted to increase, as seen in the numerical solution, and at $f = 1.29$ bifurcates into two non-oscillatory modes. This compares to a numerical value of $f = 1.16$.

Figures 5-7 show a series of results on the linear stability spectrum corresponding to two-dimensional low-frequency disturbances. Figure 5 shows a comparison of the migration of the growth rate $\mathrm{Re}(\lambda)$ and frequency $\mathrm{Im}(\lambda)$ with wavenumber k for the two-dimensional low-frequency mode as predicted by the asymptotic analysis above against a direct numerical solution of the exact linear stability spectrum (Short 1996a) for $Q = 50$, $E = 100$, $\gamma = 1.2$ and $f = 1.2$. For $k = 0$, both predict the presence of two non-oscillatory modes. For $k > 0$, the asymptotic solution predicts that the growth rate of the smaller mode increases, while that of the larger mode decreases. At $k = 0.53$, the two non-oscillatory modes merge into a single oscillatory mode with a growth rate $\mathrm{Re}(\lambda) = 0.68$ at $k = 0.53$. The growth rate of this oscillatory mode then increases slightly with increasing k reaching a maximum at $k = 0.76$, before decaying and ultimately stabilizing at a value $k = 3.17$. Thus stability is predicted for large enough wavenumbers. The direct numerical solution closely mimics this behaviour, predicting a merging of the non-oscillatory modes at $k = 0.67$, with stability occurring at $k = 3.05$.

Figure 6 shows a comparison of the migration of the growth rate $\mathrm{Re}(\lambda)$ and frequency $\mathrm{Im}(\lambda)$ with wavenumber k for the two-dimensional low-frequency mode predicted by the asymptotic solution above against a direct numerical solution of the linear stability spectrum (Short 1996a) for $Q = 50$, $E = 50$, $\gamma = 1.2$ and $f = 1$, i.e. with the steady detonation wave running at the

Chapman-Jouguet velocity. The two-dimensional asymptotic dispersion relation is then obtained from the compatibility relation (123). Figure 6 shows qualitatively identical behaviour to that observed in figure 5. The two non-oscillatory modes present for $k = 0$ in both the asymptotic and numerical solutions merge into a single non-oscillatory mode at $k = 0.42$ (asymptotic) and $k = 0.29$ (numerical). In both cases the growth rate of the oscillatory mode is observed to increase with increasing k, reaching a maximum at $k = 1.31$ (asymptotic) and $k = 0.82$ (numerical) before decaying and stabilizing at $k = 3.95$ (asymptotic) and $k = 2.77$ (numerical). Thus the asymptotic solution predicts that the detonation will be stable to low-frequency disturbances with a sufficiently large wavenumber. Moreover, it selects a maximum growth rate $\mathrm{Re}(\lambda) = 0.78$ at a critical wavenumber $k = 1.31$.

This latter finding is of interest in light of the recent work of Short and Stewart (1996), who have conjectured that rather like the situation found in direct numerical simulations of one-dimensional pulsating instability, where for a range of parameters the pulsation frequency corresponds to that of the lowest frequency linearly unstable mode, a similar situation might exist in two-dimensional cellular detonation simulations. More specifically, it has been proposed that for a range of detonation parameters, the cell width observed in direct two-dimensional simulations might correspond to the wavenumber associated with the maximum growth rate of the *lowest* frequency oscillatory mode found in the linear stability analysis. Thus although there might be larger growth rates corresponding to higher frequency disturbances in the linear stability spectra, it is the former which will determine the cell size in the unstable two-dimensional detonation propagation. Further work is currently underway in order to clarify any link. However, if this conjecture proves to be correct then the present asymptotic theory provides a mechanism for predicting the cell size.

Finally, fig. 7 is a plot of the migration of the growth rates and frequencies with wavenumber k of three low-frequency modes of instability as predicted by the asymptotic analysis for $Q = 50$, $E = 50$, $\gamma = 1.2$ and $f = 1.3$ (solid lines), $f = 1.4$ (dotted lines) and $f = 1.5$ (dashed lines). All modes are oscillatory. For each mode, the growth rate increases with increasing wavenumber k reaching a maximum at $k = 1.44$ ($f = 1.3$), $k = 1.49$ ($f = 1.4$) and $k = 1.53$ ($f = 1.5$). After reaching the maximum, the growth rate of each mode decays with increasing k, before stabilizing at $k = 3.94$ ($f = 1.3$), $k = 3.92$ ($f = 1.4$) and $k = 3.90$ ($f = 1.5$). Thus the asymptotic analysis again selects a critical wavenumber for each low-frequency mode corresponding to a maximum growth rate in the linear stability spectrum.

6. Summary

We have derived a wholly analytical dispersion relation governing the low-frequency two-dimensional linear stability of a plane detonation wave which is travelling at the Chapman-Jouguet detonation speed or is overdriven. This asymptotic analysis employs the limit of high activation energy and the Newtonian limit, in which $\gamma \to 1$. The dispersion relation retains a dependence on the activation energy, and comparisons with exact numerical solutions of the low-

frequency linear stability spectrum are excellent. The mechanism governing the low-frequency linear instability of detonation are highlighted and is shown to involve a complex interaction between acoustic wave disturbances and entropy changes in the induction zone of the detonation. Simplified forms of the dispersion relation and weakly non-linear evolution equations corresponding to these relations, together with the recovery of the results of Buckmaster and Ludford (1987) when $\lambda \sim O(1/\theta)$, $k \sim O(1/\theta)$, Buckmaster (1989) when $\lambda \sim O(1/\theta)$, $k \sim O(1/\sqrt{\theta})$, and Short (1996) when $\lambda \sim O(1)$, $k \sim O(1)$, will be investigated in a future article, where a more detailed examination of the mechanism governing the linear instability will also be presented.

Acknowledgements

MS was supported by an Engineering and Physical Sciences Research Council research grant. DSS was supported by U.S. Air Force Wright Laboratories, Armament Directorate (F08630-94-10004), the U.S. Air Force Office of Scientific Research, Mathematics (F496-93-1-0532) and the U.S. Department of Energy, Los Alamos National Laboratories.

References

[1] G. ABOUSEIF & T.Y. TOONG, *Theory of unstable one-dimensional detonations,* Combust. Flame **45** (1982) 64–94.

[2] R.L. ALPERT & T.Y. TOONG, *Periodicity in exothermic hypersonic flows about blunt projectiles,* Astron. Acta **17** (1972) 539–560.

[3] P. BLYTHE AND D. CRIGHTON, *Shock Generated Ignition: the induction zone,* Proc. R. Soc. Lond. A **426** (1989) 189–209.

[4] A. BOURLIOUX, A.J. MAJDA & V. ROYTBURD, *Theoretical and numerical structure for unstable one-dimensional detonations,* SIAM J. Appl. Math. **51** (1991) 303–343.

[5] A. BOURLIOUX & A.J. MAJDA, *Theoretical and numerical structure for unstable two-dimensional detonations,* Comb. and Flame **90** (1992) 211–229.

[6] J.D. BUCKMASTER & G.S.S LUDFORD, *The effect of structure on the stability of detonations I. Role of the induction zone,* Twenty-first Symposium (International) on Combustion, The Combustion Institute, Pittsburgh, 1987, pp. 1669–1676.

[7] J.D. BUCKMASTER & J. NEVIS, *One-dimensional detonation stability: The spectrum for infinite activation energy,* Phys. Fluids **31** (1988) 3571–3576.

[8] J.D. BUCKMASTER, *A theory for triple point spacing in overdriven detonation waves,* Comb. and Flame **77** (1989) 219–228.

[9] J.F. CLARKE, *Finite Amplitude Waves in Combustible Gases,* in 'The Mathematics of Combustion,' J.D. Buckmaster, Ed., SIAM Publications, Philadelphia, 1985, pp. 183–245.

[10] J.J. ERPENBECK, *Stability of idealized one-reaction detonations,* Phys. Fluids **7** (1964) 684–696.

[11] J.J. ERPENBECK, *Structure and stability of the square-wave detonation,* Ninth Symposium (International) on Combustion, The Combustion Institute, New York, Academic Press, (1963), pp. 442–453.

[12] W. FICKETT & W. W. WOOD *Flow calculations for pulsating one-dimensional detonations,* Phys. Fluids **9** (1966) 903–916.

[13] H.I. LEE & D.S. STEWART, *Calculation of linear instability: one-dimensional instability of plane detonation,* J. Fluid Mech. **216** (1990) 103–132.

[14] J.J. QUIRK, *Godunov-type schemes applied to detonation flows,* in Combustion in high-speed flows (Eds. J. Buckmaster, T.L. Jackson, A. Kumar), (1994) pp. 575–596.

[15] J.J. QUIRK, *A parallel adaptive mesh refinement algorithm for computational shock hydrodynamics,* Appl. Num. Math. (1995) in press.

[16] J.J. QUIRK & M. SHORT, *Nonlinear stability analysis of one-dimensional detonation,* in preparation.

[17] M. SHORT, *Multi-dimensional linear stability of a detonation wave at high-activation energy,* SIAM J. Appl. Math., in press, 1996a.

[18] M. SHORT, *An asymptotic estimate of the linear stability of the square wave detonation using the Newtonian limit,* Proc. Roy. Soc. A., in press, 1996b.

[19] M. SHORT & D.S. STEWART, *Two-dimensional linear instability of a plane detonation wave,* submitted, 1996.

[20] D. S. STEWART, T.D. ASLAM & YAO J., *On the evolution of cellular detonation,* University of Illinois, TAM Report No. 775, UILU-ENG 64-6031, November (1996), submitted to the 26th (International) Symposium on Combustion, Naples 1996.

[21] R.A. STREHLOW, *Multi-dimensional detonation wave structure,* Astro. Acta **15** (1970) 345-357.

[22] J. YAO AND D.S. STEWART, *On the dynamics of multi-dimensional detonation waves,* J. Fluid Mech. **309** (1996) 225-275.

[23] R.M. ZAIDEL, *The stability of detonation waves in gaseous detonations,* Dokl. Akad. Nauk SSSR (Phys. Chem Sect.) **136** (1961) 1142–1145.

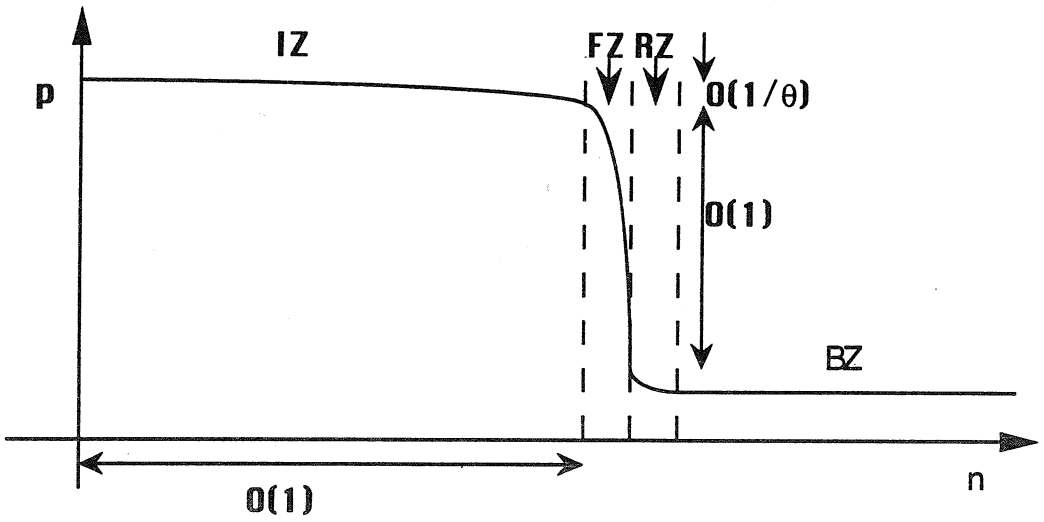

Figure 1: Structure of the steady square wave detonation. The induction zone, fire zone, relaxation zone and equilibrium (or burnt) zone are denoted by IZ, FZ, RZ and BZ respectively.

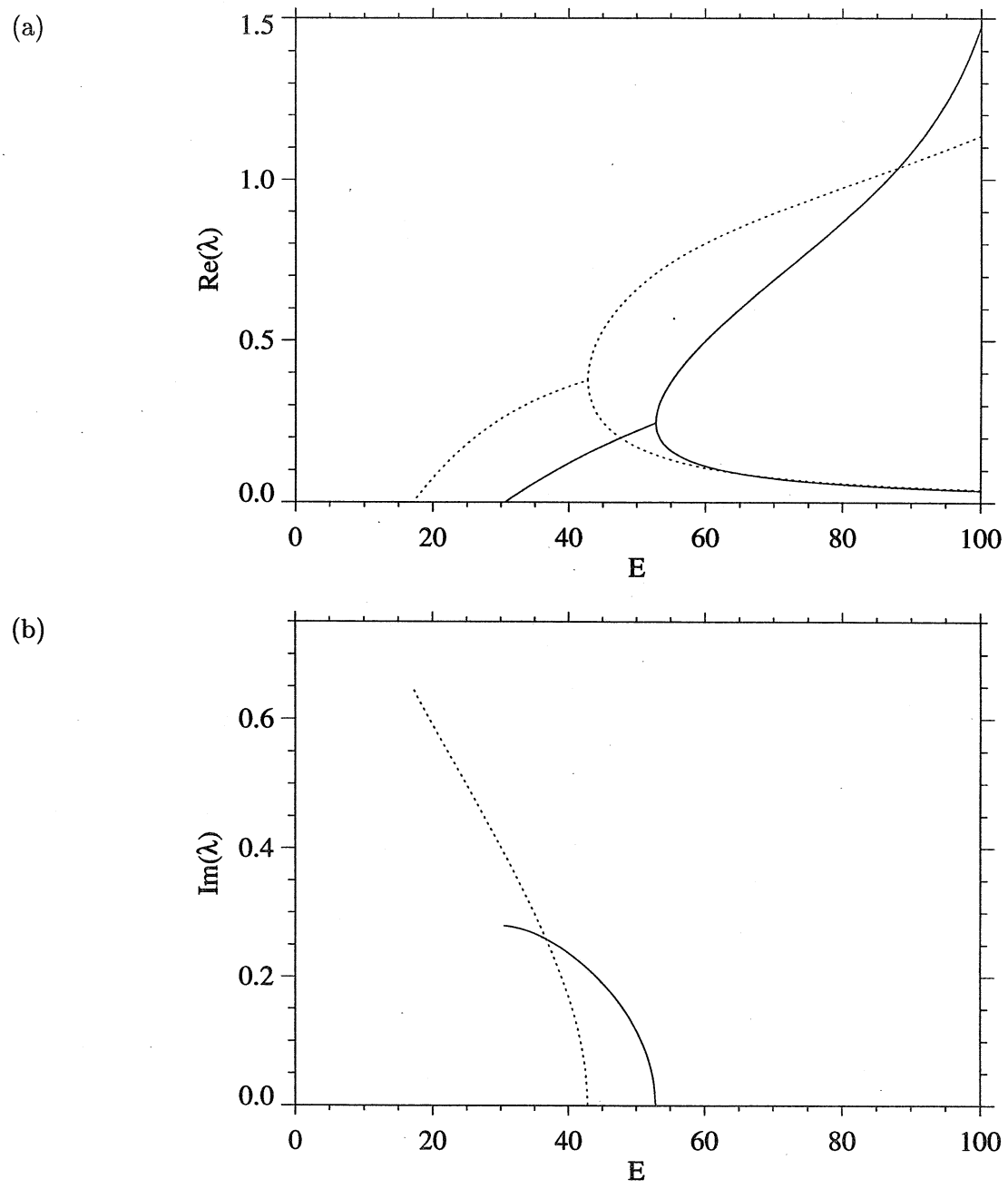

Figure 2: The migration of (a) the growth rate $\mathrm{Re}(\lambda)$ and (b) the frequency $\mathrm{Im}(\lambda)$ with activation E of the one-dimensional low-frequency linear disturbance as calculated numerically in Short (1996a) (solid lines) and asymptotically (dotted lines) from (119-121) and (112) with $Q = 50$, $\gamma = 1.2$ and $f = 1.2$.

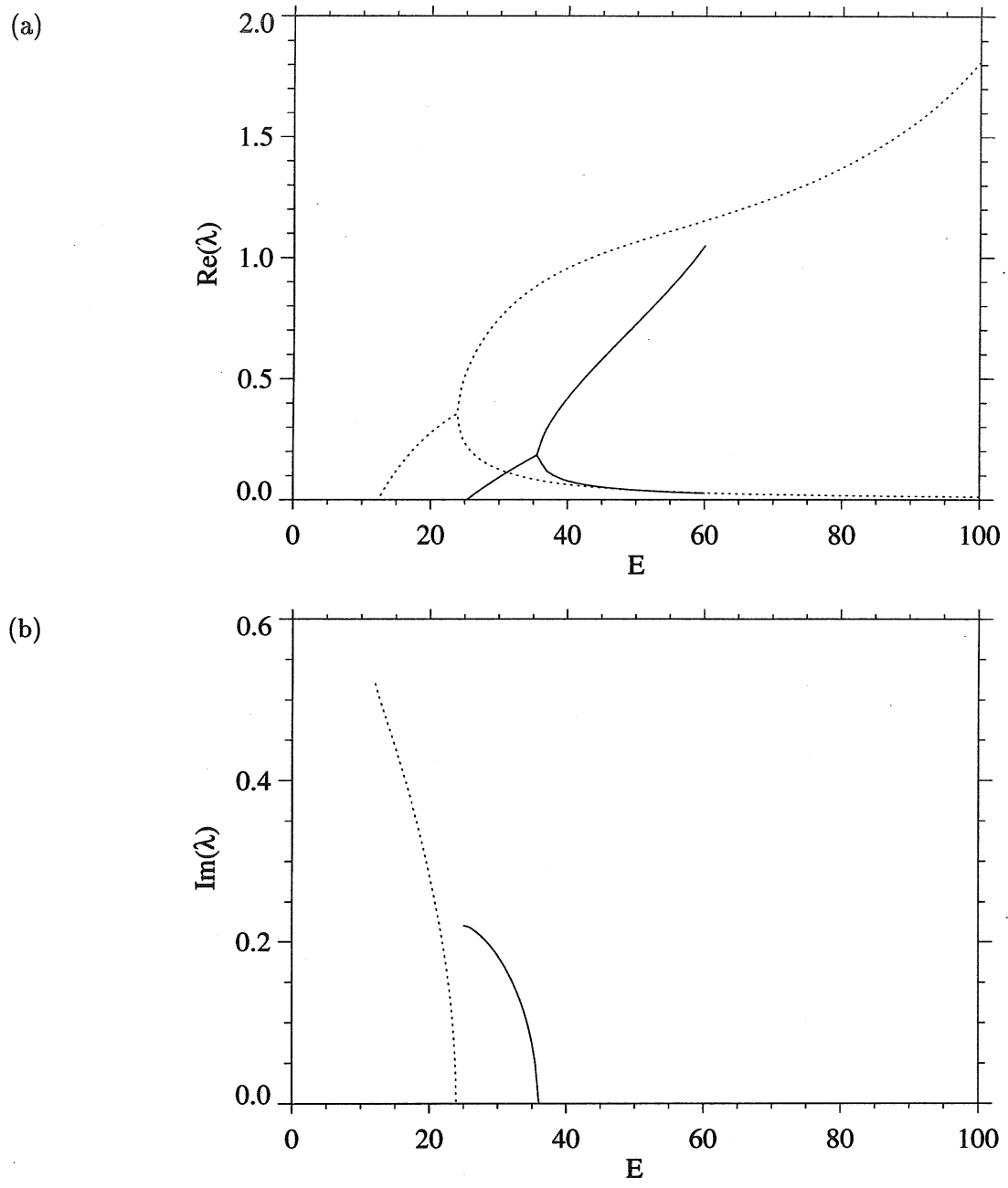

Figure 3: The migration of (a) the growth rate $\mathrm{Re}(\lambda)$ and (b) the frequency $\mathrm{Im}(\lambda)$ with activation E of the one-dimensional low-frequency linear disturbance as calculated numerically in Short (1996a) (solid lines) and asymptotically (dotted lines) from (123) with $Q = 50$, $\gamma = 1.2$ and $f = 1.0$.

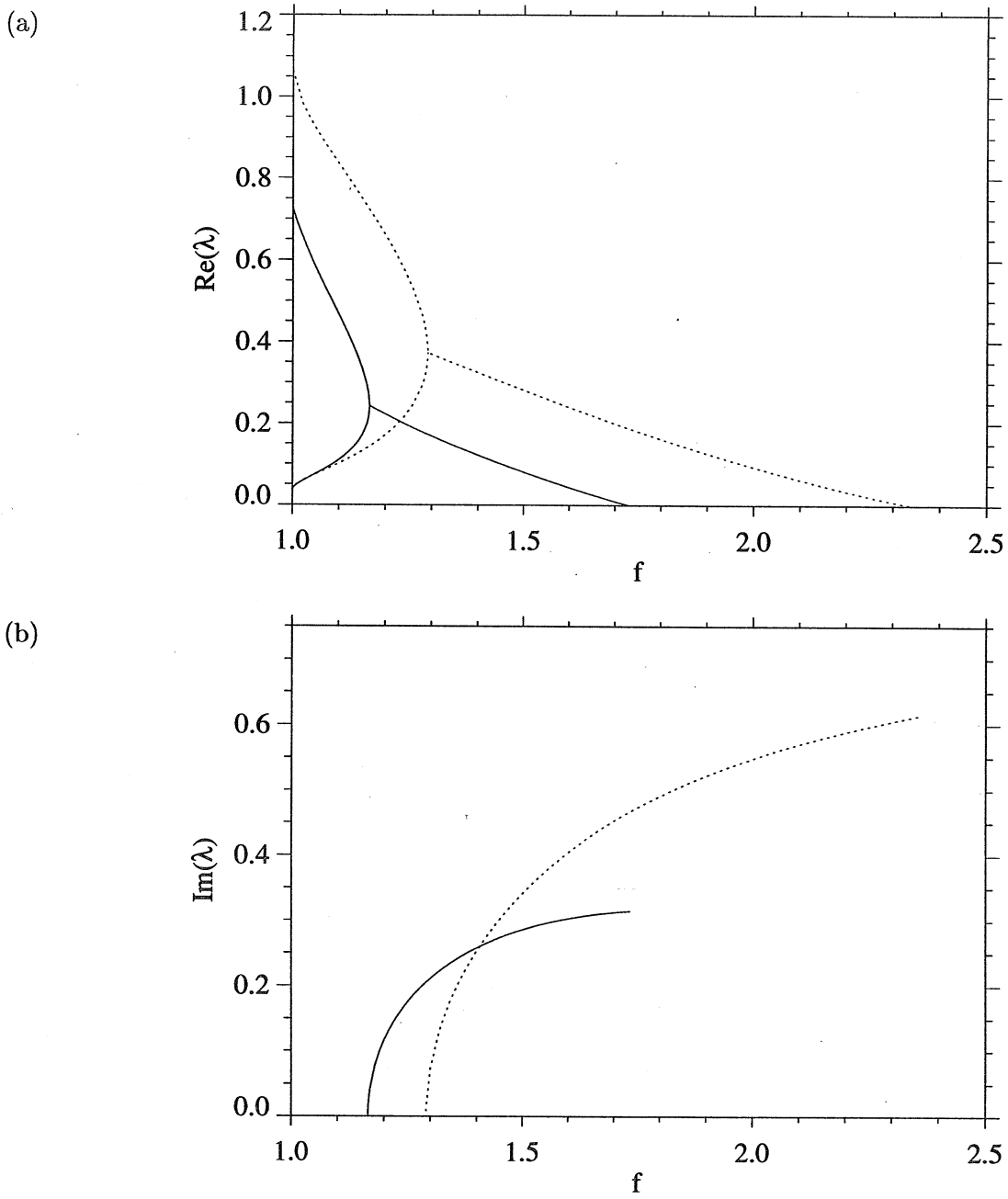

Figure 4: The migration of (a) the growth rate $\mathrm{Re}(\lambda)$ and (b) the frequency $\mathrm{Im}(\lambda)$ with overdrive f of the one-dimensional low-frequency linear disturbance as calculated numerically in Short (1996a) (solid lines) and asymptotically (dotted lines) from (119-121) and (112) when $f > 1$ and (123) when $f = 1$ with $Q = 50$, $E = 50$ and $\gamma = 1.2$.

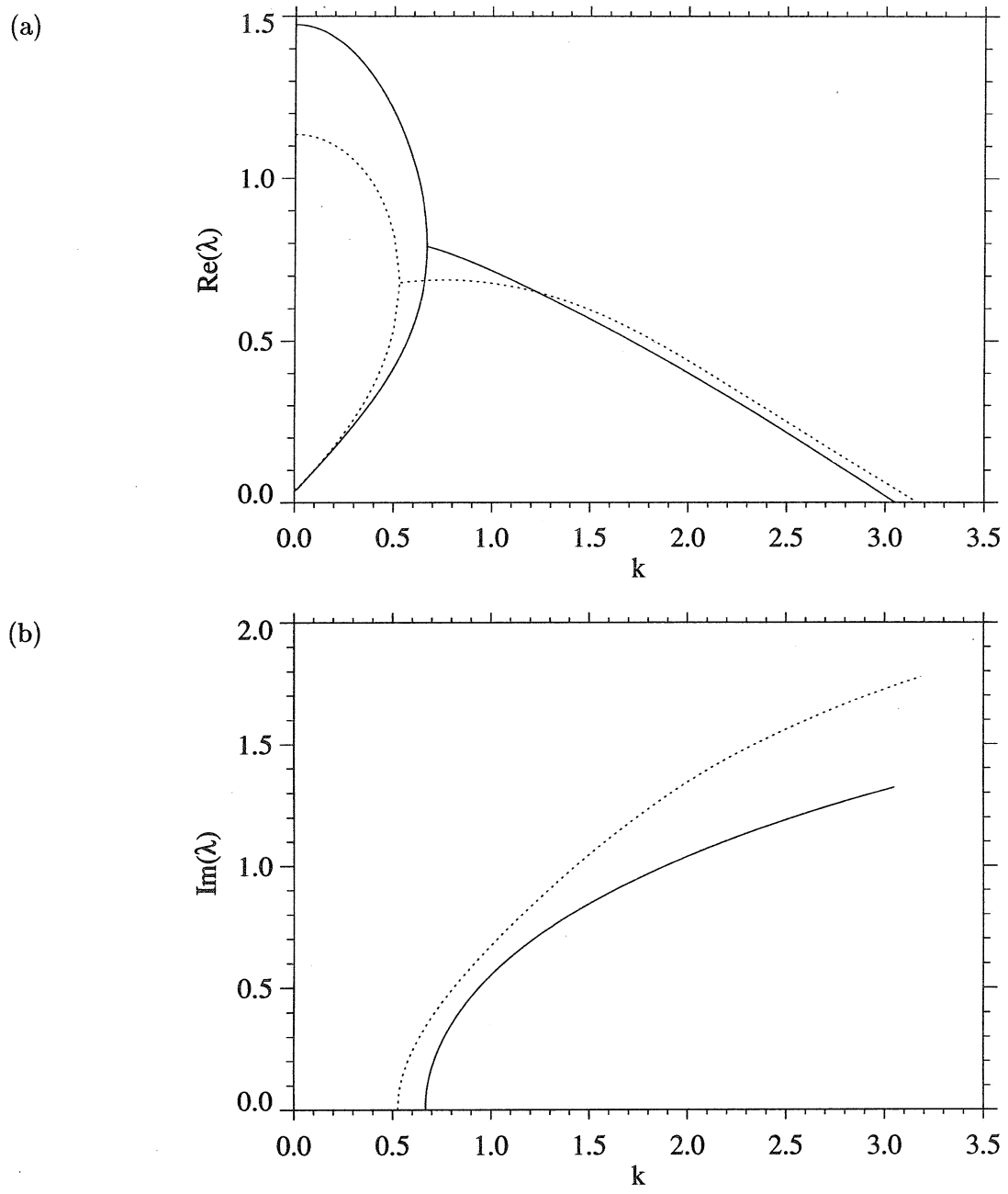

Figure 5: The migration of (a) the growth rate $\mathrm{Re}(\lambda)$ and (b) the frequency $\mathrm{Im}(\lambda)$ with wavenumber κ of the two-dimensional low-frequency linear disturbance as calculated numerically in Short (1996a) (solid lines) and asymptotically (dotted lines) from (119-121) and (112) with $Q = 50$, $E = 100$ and $\gamma = 1.2$ and $f = 1.2$.

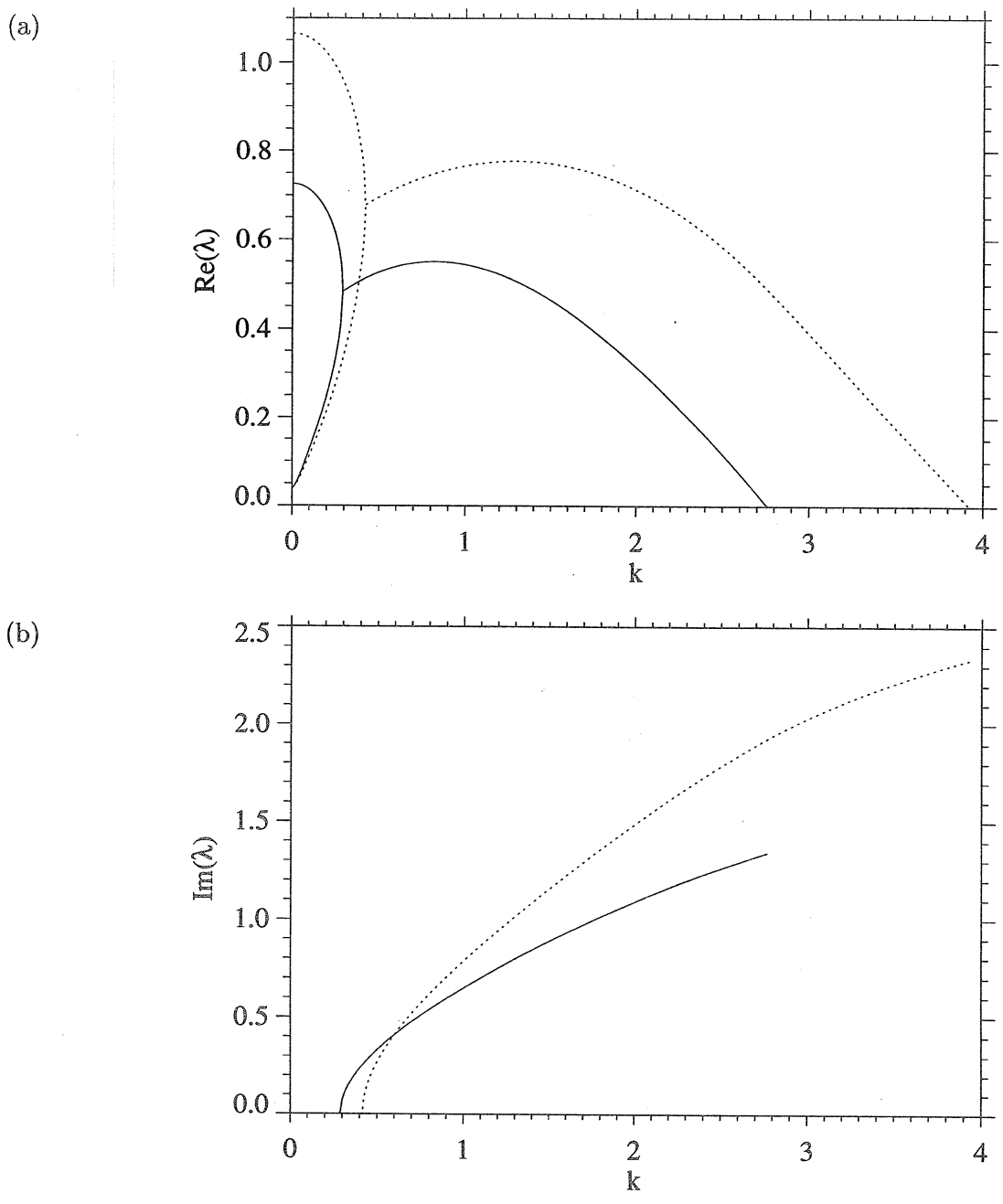

Figure 6: The migration of (a) the growth rate $\mathrm{Re}(\lambda)$ and (b) the frequency $\mathrm{Im}(\lambda)$ with wavenumber κ of the two-dimensional low-frequency linear disturbance as calculated numerically in Short (1996a) (solid lines) and asymptotically (dotted lines) from (123) with $Q = 50$, $E = 50$ and $\gamma = 1.2$ and $f = 1$.

(a)

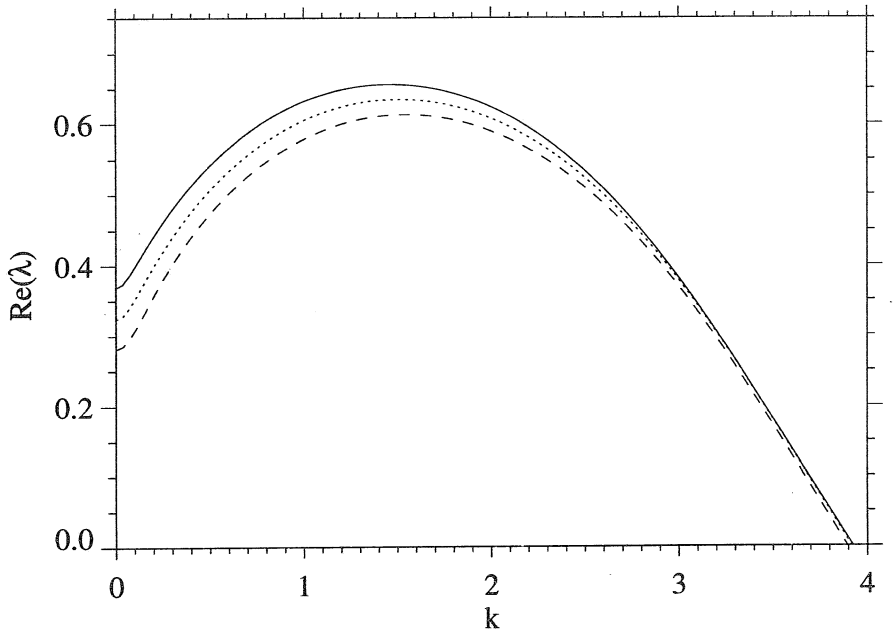

(b)

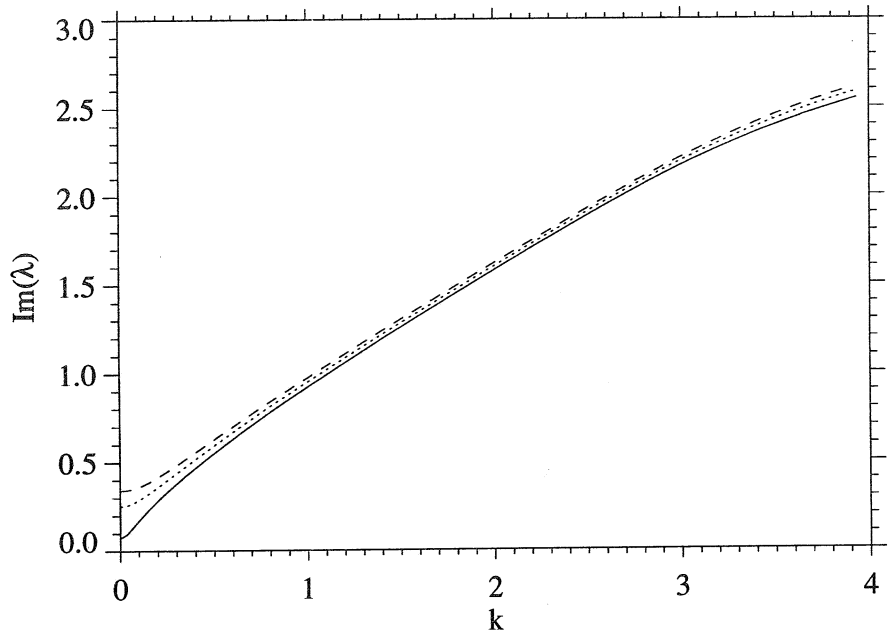

Figure 7: The migration of the growth rate $\mathrm{Re}(\lambda)$ and frequency $\mathrm{Im}(\lambda)$ with wavenumber κ of the two-dimensional low-frequency linear disturbance as calculated asymptotically from (119-121) and (121) with $Q = 50$, $E = 50$ and $\gamma = 1.2$ and with $f = 1.3$ (solid line), $f = 1.4$ (dotted line) and $f = 1.5$ (dashed line).

List of Recent TAM Reports

No.	Authors	Title	Date
740	Weaver, R. L., W. Sachse, and K. Y. Kim	Transient elastic waves in a transversely isotropic plate—*Journal of Applied Mechanics*, in press (1996)	Dec. 1993
741	Zhang, Y., and R. L. Weaver	Scattering from a thin random fluid layer—*Journal of the Acoustical Society of America* **96**, 1899–1909 (1994)	Dec. 1993
742	Weaver, R. L., and W. Sachse	Diffusion of ultrasound in a glass bead slurry—*Journal of the Acoustical Society of America* **97**, 2094–2102 (1995)	Dec. 1993
743	Sundermeyer, J. N., and R. L. Weaver	On crack identification and characterization in a beam by nonlinear vibration analysis—*Journal of Sound and Vibration* **183**, 857–872 (1995)	Dec. 1993
744	Li, L., and N. R. Sottos	Predictions of static displacements in 1–3 piezocomposites—*Journal of Intelligent Materials Systems and Structures* **6**, 169–180 (1995)	Dec. 1993
745	Jones, S. W.	Chaotic advection and dispersion—*Physica D* **76**, 55–69 (1994)	Jan. 1994
746	Stewart, D. S., and J. Yao	Critical detonation shock curvature and failure dynamics: Developments in the theory of detonation shock dynamics—*Developments in Theoretical and Applied Mechanics* **17** (1994)	Feb. 1994
747	Mei, R., and R. J. Adrian	Effect of Reynolds-number-dependent turbulence structure on the dispersion of fluid and particles—*Journal of Fluids Engineering* **117**, 402-409 (1995)	Feb. 1994
748	Liu, Z.-C., R. J. Adrian, and T. J. Hanratty	Reynolds-number similarity of orthogonal decomposition of the outer layer of turbulent wall flow—*Physics of Fluids* **6**, 2815–2819 (1994)	Feb. 1994
749	Barnhart, D. H., R. J. Adrian, and G. C. Papen	Phase-conjugate holographic system for high-resolution particle image velocimetry—*Applied Optics* **33**, 7159–7170 (1994)	Feb. 1994
750	Qi, Q., W. D. O'Brien Jr., and J. G. Harris	The propagation of ultrasonic waves through a bubbly liquid into tissue: A linear analysis—*IEEE Transactions on Ultrasonics, Ferroelectrics and Frequency Control* **42**, 28–36 (1995)	Mar. 1994
751	Mittal, R., and S. Balachandar	Direct numerical simulation of flow past elliptic cylinders—*Journal of Computational Mechanics*, in press (1996)	May 1994
752	Students in TAM 293–294	Thirty-first student symposium on engineering mechanics, J. W. Phillips, coordinator: Selected senior projects by D. N. Anderson, J. R. Dahlen, M. J. Danyluk, A. M. Dreyer, K. M. Durkin, J. J. Kriegsmann, J. T. McGonigle, and V. Tyagi	May 1994
753	Thoroddsen, S. T.	The failure of the Kolmogorov refined similarity hypothesis in fluid turbulence—*Physics of Fluids* **7**, 691–693 (1995)	May 1994
754	Turner, J. A., and R. L. Weaver	Time dependence of multiply scattered diffuse ultrasound in polycrystalline media—*Journal of the Acoustical Society of America* **97**, 2639–2644 (1995)	June 1994
755	Riahi, D. N.	Finite-amplitude thermal convection with spatially modulated boundary temperatures—*Proceedings of the Royal Society of London A* **449**, 459–478 (1995)	June 1994
756	Riahi, D. N.	Renormalization group analysis for stratified turbulence—*International Journal of Mathematics and Mathematical Sciences*, in press (1996)	June 1994
757	Riahi, D. N.	Wave-packet convection in a porous layer with boundary imperfections—*Journal of Fluid Mechanics*, in press (1996)	June 1994
758	Jog, C. S., and R. B. Haber	Stability of finite element models for distributed-parameter optimization and topology design—*Computer Methods in Applied Mechanics and Engineering*, in press (1996).	July 1994

List of Recent TAM Reports (cont'd)

No.	Authors	Title	Date
759	Qi, Q., and G. J. Brereton	Mechanisms of removal of micron-sized particles by high-frequency ultrasonic waves—*IEEE Transactions on Ultrasonics, Ferroelectrics and Frequency Control* **42**, 619–629 (1995)	July 1994
760	Shawki, T. G.	On shear flow localization with traction-controlled boundaries—*International Journal of Solids and Structures* **32**, 2751–2778 (1995)	July 1994
761	Balachandar, S., D. A. Yuen, and D. M. Reuteler	High Rayleigh number convection at infinite Prandtl number with temperature-dependent viscosity	July 1994
762	Phillips, J. W.	Arthur Newell Talbot—Proceedings of a conference to honor TAM's first department head and his family	Aug. 1994
763	Man., C. S., and D. E. Carlson	On the traction problem of dead loading in linear elasticity with initial stress—*Archive for Rational Mechanics and Analysis* **128**, 223–247 (1994)	Aug. 1994
764	Zhang, Y., and R. L. Weaver	Leaky Rayleigh wave scattering from elastic media with random microstructures	Aug. 1994
765	Cortese, T. A., and S. Balachandar	High-performance spectral simulation of turbulent flows in massively parallel machines with distributed memory—*International Journal of Supercomputer Applications* **9**, 185–202 (1995)	Aug. 1994
766	Balachandar, S.	Signature of the transition zone in the tomographic results extracted through the eigenfunctions of the two-point correlation—*Geophysical Research Letters* **22**, 1941–1944 (1995)	Sept. 1994
767	Piomelli, U.	Large-eddy simulation of turbulent flows	Sept. 1994
768	Harris, J. G., D. A. Rebinsky, and G. R. Wickham	An integrated model of scattering from an imperfect interface—*Journal of the Acoustical Society of America*, in press (1996)	Sept. 1994
769	Hsia, K. J., and Z.-Q. Xu	The mathematical framework and an approximate solution of surface crack propagation under hydraulic pressure loading—*International Journal of Fracture*, in press (1996)	Sept. 1994
770	Balachandar, S.	Two-point correlation and its eigen-decomposition for optimal characterization of mantle convection	Oct. 1994
771	Lufrano, J. M., and P. Sofronis	Numerical analysis of the interaction of solute hydrogen atoms with the stress field of a crack—*International Journal of Solids and Structures*, in press (1996)	Oct. 1994
772	Aref, H., and S. W. Jones	Motion of a solid body through ideal fluid	Oct. 1994
773	Stewart, D. S., T. D. Aslam, J. Yao, and J. B. Bdzil	Level-set techniques applied to unsteady detonation propagation—In "Modeling in Combustion Science," *Lecture Notes in Physics* (1995)	Oct. 1994
774	Mittal, R., and S. Balachandar	Effect of three-dimensionality on the lift and drag of circular and elliptic cylinders—*Physics of Fluids* **7**, 1841–1865 (1995)	Oct. 1994
775	Stewart, D. S., T. D. Aslam, and J. Yao	On the evolution of cellular detonation	Nov. 1994 *Revised* Jan. 1996
776	Aref, H.	On the equilibrium and stability of a row of point vortices—*Journal of Fluid Mechanics* **290**, 167–181 (1995)	Nov. 1994
777	Cherukuri, H. P., T. G. Shawki, and M. El-Raheb	An accurate finite-difference scheme for elastic wave propagation in a circular disk—*Journal of the Acoustical Society of America*, in press (1996)	Nov. 1994
778	Li, L., and N. R. Sottos	Improving hydrostatic performance of 1–3 piezocomposites—*Journal of Applied Physics* **77**, 4595–4603 (1995)	Dec. 1994

No.	Authors	Title	Date
779	Phillips, J. W., D. L. de Camara, M. D. Lockwood, and W. C. C. Grebner	Strength of silicone breast implants—*Plastic and Reconstructive Surgery* **97**, in press (1996)	Jan. 1995
780	Xin, Y.-B., K. J. Hsia, and D. A. Lange	Quantitative characterization of the fracture surface of silicon single crystals by confocal microscopy—*Journal of the American Ceramics Society* **78**, 3201-3208 (1995)	Jan. 1995
781	Yao, J., and D. S. Stewart	On the dynamics of multi-dimensional detonation—*Journal of Fluid Mechanics* **309**, 225-275 (1996)	Jan. 1995
782	Riahi, D. N., and T. L. Sayre	Effect of rotation on the structure of a convecting mushy layer—*Acta Mechanica*, in press (1996)	Feb. 1995
783	Batchelor, G. K., and TAM faculty and students	A conversation with Professor George K. Batchelor	Feb. 1995
784	Sayre, T. L., and D. N. Riahi	Effect of rotation on flow instabilities during solidification of a binary alloy	Feb. 1995
785	Xin, Y.-B., and K. J. Hsia	A technique to generate straight surface cracks for studying the dislocation nucleation condition in brittle materials —*Acta Metallurgica et Materialia* **44**, 845-853 (1996).	Mar. 1995
786	Riahi, D. N.	Finite bandwidth, long wavelength convection with boundary imperfections: Near-resonant wavelength excitation	Mar. 1995
787	Turner, J. A., and R. L. Weaver	Average response of an infinite plate on a random foundation—*Journal of the Acoustical Society of America* **99**, in press (1996)	Mar. 1995
788	Weaver, R. L., and D. Sornette	The range of spectral correlations in pseudointegrable systems: GOE statistics in a rectangular membrane with a point scatterer—*Physical Review E* **52**, 341 (1995)	April 1995
789	Students in TAM 293–294	Thirty-second student symposium on engineering mechanics, J. W. Phillips, coordinator: Selected senior projects by K. F. Anderson, M. B. Bishop, B. C. Case, S. R. McFarlin, J. M. Nowakowski, D. W. Peterson, C. V. Robertson, and C. E. Tsoukatos	April 1995
790	Figa, J., and C. J. Lawrence	Linear stability analysis of a gravity-driven Newtonian coating flow on a planar incline	May 1995
791	Figa, J., and C. J. Lawrence	Linear stability analysis of a gravity-driven viscosity-stratified Newtonian coating flow on a planar incline	May 1995
792	Cherukuri, H. P., and T. G. Shawki	On shear band nucleation and the finite propagation speed of thermal disturbances—*International Journal of Solids and Structures*, in press (1996)	May 1995
793	Harris, J. G.	Modeling scanned acoustic imaging of defects at solid interfaces—Chapter in *IMA Workshop on Inverse Problems in Wave Propagation*, Springer-Verlag, in press (1996)	May 1995
794	Sottos, N. R., J. M. Ockers, and M. J. Swindeman	Thermoelastic properties of plain weave composites for multilayer circuit board applications	May 1995
795	Aref, H., and M. A. Stremler	On the motion of three point vortices in a periodic strip—*Journal of Fluid Mechanics*, in press (1996).	June 1995
796	Barenblatt, G. I., and N. Goldenfeld	Does fully-developed turbulence exist? Reynolds number independence versus asymptotic covariance—*Physics of Fluids* **7**, 3078–3082 (1995)	June 1995
797	Aslam, T. D., J. B. Bdzil, and D. S. Stewart	Level set methods applied to modeling detonation shock dynamics—*Journal of Computational Physics*, in press (1996)	June 1995

List of Recent TAM Reports (cont'd)

No.	*Authors*	*Title*	*Date*
798	Nimmagadda, P. B. R., and P. Sofronis	The effect of interface slip and diffusion on the creep strength of fiber and particulate composite materials—*Mechanics of Materials,* in press (1996)	July 1995
799	Hsia, K. J., T.-L. Zhang, and D. F. Socie	Effect of crack surface morphology on the fracture behavior under mixed mode loading —*ASTM Special Technical Publication* 1296, in press (1996)	July 1995
800	Adrian, R. J.	Stochastic estimation of the structure of turbulent fields	Aug. 1995
801	Riahi, D. N.	Perturbation analysis and modeling for stratified turbulence	Aug. 1995
802	Thoroddsen, S. T.	Conditional sampling of dissipation in high Reynolds number turbulence —*Physics of Fluids,* in press (1996)	Aug. 1995
803	Riahi, D. N.	On the structure of an unsteady convecting mushy layer	Aug. 1995
804	Meleshko, V. V.	Equilibrium of an elastic rectangle: The Mathieu–Inglis–Pickett solution revisited—*Journal of Elasticity* **40**, 207-238 (1995)	Aug. 1995
805	Jonnalagadda, K., G. E. Kline, and N. R. Sottos	Local displacements and load transfer in shape memory alloy composites	Aug. 1995
806	Nimmagadda, P. B. R., and P. Sofronis	On the calculation of the matrix–reinforcement interface diffusion coefficient in composite materials at high temperatures—*Acta Metallurgica et Materialia*, in press (1996)	Aug. 1995
807	Carlson, D. E., and D. A. Tortorelli	On hyperelasticity with internal constraints—*Journal of Elasticity*, in press (1996)	Aug. 1995
808	Sayre, T. L., and D. N. Riahi	Oscillatory instabilities of the liquid and mushy layers during solidification of alloys under rotational constraint—*Acta Mechanica,* in press (1996)	Sept. 1995
809	Xin, Y.-B., and K. J. Hsia	Simulation of the brittle-ductile transition in silicon single crystals using dislocation mechanics	Oct. 1995
810	Ulysse, P., and R. E. Johnson	A plane-strain upper-bound analysis of unsymmetrical single-hole and multi-hole extrusion processes	Oct. 1995
811	Fried, E.	Continua described by a microstructural field—*Zeitschrift für angewandte Mathematik und Physik,* in press (1996)	Nov. 1995
812	Mittal, R., and S. Balachandar	Autogeneration of three-dimensional vortical structures in the near wake of a circular cylinder	Nov. 1995
813	Segev, R., E. Fried, and G. de Botton	Force theory for multiphase bodies—*Journal of Geometry and Physics*, in press (1996)	Dec. 1995
814	Weaver, R. L.	The effect of an undamped finite-degree-of-freedom "fuzzy" substructure: Numerical solutions and theoretical discussion	Jan. 1996
815	Haber, R. B., C. S. Jog, and M. P. Bensøe	A new approach to variable-topology shape design using a constraint on perimeter—*Structural Optimization* **11**, 1-12 (1996)	Feb. 1996
816	Xu, Z.-Q., and K. J. Hsia	A numerical solution of a surface crack under cyclic hydraulic pressure loading	Mar. 1996
817	Adrian, R. J.	Bibliography of particle velocimetry using imaging methods: 1917–1995—*Produced and distributed in cooperation with TSI, Inc., St. Paul, Minn.*	Mar. 1996
818	Fried, E., and G. Grach	An order-parameter based theory as a regularization of a sharp-interface theory for solid–solid phase transitions—*Archive for Rational Mechanics and Analysis,* in press (1996)	Mar. 1996
819	Vonderwell, M. P., and D. N. Riahi	Resonant instability mode triads in the compressible boundary-layer flow over a swept wing	Mar. 1996
820	Short, M., and D. S. Stewart	Low-frequency two-dimensional linear instability of plane detonation	Mar. 1996